

REMARKS

In view of the following remarks, the Examiner is respectfully requested to withdraw the rejections and allow claims 11, 13-15, 18, 27, 30, 31 and 34, the only claims pending and currently under examination in this application.

Formal Matters:

Claims 11, 13-15, 18, 27, 30, 31 and 34 are pending after entry of the amendments set forth herein.

Claims 1-10 and 19-26 were previously canceled without prejudice.

For the sole purpose of expediting prosecution, Applicant hereby cancels claims 12, 16, 17, 28, 29, 32, 33 and 35-41. Applicant reserve the right to prosecute the subject matter covered by these claims in another continuation application.

Claims 11, 14, 18, 27, 30, 31 and 34 are amended. Support for these amendments is found throughout the specification and in the claims as originally filed.

Claim Rejections – 35 U.S.C. § 112, first paragraph

Written Description

Claims 12 and 35 -41 have been rejected under 35 U.S.C. § 112, first paragraph, as allegedly failing to comply with the written description requirement. As claims 12 and 35-41 are hereby canceled, this rejection is rendered moot.

Enablement

Claims 11, 13-15, 18, 27, 30, 31 and 34 remain rejected under 35 U.S.C. § 112, first paragraph on the basis that the specification allegedly does not enable a person skilled in the art to which it pertains, or which it is most closely connected, to make and use the claimed invention commensurate in scope with the claims. The Applicant respectfully traverses this rejection as it is applied to the pending claims. As claims 12, 16, 17, 28, 29, 32 and 33 are canceled, the rejection of these claims is rendered moot.

The Examiner acknowledges that enablement is present for a method of inserting an exogenous nucleic acid into the genome of a **mouse**, wherein the method comprises introducing into the **mouse** a P-element derived vector comprising a pair of P-elements transposase recognized insertion sequences flanking at least one transcriptionally active gene that is at least 50 bp proximity to one of the P-element transposase recognized sequences, wherein a transposase domain is provided on the same vector or a second P-element vector, and cells from the **mouse**. However, the Examiner alleges that the specification does not provide enablement for making any transgenic animal, other than a mouse, commensurate with the scope of the claims.

Amended claims 11 and 13-15 are directed to a method of inserting an exogenous nucleic acid into the genome of a **rodent**. Amended claim 18 is directed a method of inserting an exogenous nucleic acid into the genome of a **mouse**. Amended claims 27 and 31 are directed a **rodent** or cells derived from a **rodent**. Amended claims 30 and 34 are directed a **mouse** or **mouse** cells.

The law regarding enablement of inventions is: “[t]he test of enablement is whether one reasonably skilled in the art could make or use the invention from the disclosure in the patent coupled with information known in the art without undue experimentation.”¹

Disclosure of the Present Application

The Applicants maintain that the present application provides sufficient disclosure to enable the invention to the full scope of the pending claims as directed to **rodents**. The present specification clearly details the preparation and production of such transgenic rodents. Beginning on page 10, the specification provides a detailed disclosure of how to generate such rodents using the P-element derived vector and a variety of well known nucleic acid delivery techniques, as well as references describing such techniques in greater detail. The specification further provides working examples showing use of such vectors in generating transgenic rodents. Moreover, such working examples demonstrate the transgenesis of introducing the P element of a *Drosophila* fly into mice. When the Applicant demonstrated that

1. *United States v. Telectronics, Inc.*, 8 USPQ 2d 1217, 1233 (Fed. Cir. 1988), *cert. denied*, 490 U.S. 1046 (1989). See also *Genentech, Inc. v. Novo Nordisk*, 42 USPQ 2d 1001 (Fed. Cir. 1997), *cert. denied*, 522

a pair of P-element transposase recognized insertion sequences, which is derived from the *Drosophila* fly, is able to integrate into the genome of mice, the Applicant succeeded in demonstrating the genetic element of one organism is able to integrate in the genome of an unrelated organism. Both the *Drosophila* fly and the mouse are classified under the kingdom Animalia; however, the *Drosophila* fly is classified under the class Insecta of the phylum Arthropoda while the mouse is classified under the class Mammalia of the phylum Chordata. There is no reason to believe why the genetic element of an organism from one phylum should be capable of integrating into the genome of an organism of another phylum. However, the Applicant has demonstrated this application in the present specification.

In the "Response to Arguments" section, the Examiner has alleged the Applicant's arguments in the Amendment and Response dated February 27, 2006 are not persuasive. The Applicant disagrees and answers the Examiner's response point by point.

The Examiner alleges that "due to significant research in the mouse, the mouse is a model for transgenic research [and that t]hough the mouse is well characterized and studied for the purposes of transgenesis, this does not lead to a routine and easy extrapolation of science that will lead to the creation of all other transgenic non-human and non-drosophilidae animals." (page 5). The Applicant respectfully disagrees with the Examiner's reasoning. That the mouse is a well studied organism is not a rationale that a procedure used on a mouse cannot be extrapolated to other closely related organisms, such as other rodents. The specification teaches a working example of the method of introducing the vector comprising the P-element by co-injecting mice by their systemic tail vein with different concentrations of the vector and followed by a second injection of the transposase vector (page 18, lines 7-10). Rodents are genetically and morphological very similar to each other. They all belong within the order Rodentia. Injecting different concentrations of vector encoding the P-element and/or transposase into other rodents, which are closely related to the mouse, is of such simplicity that it must surely be routine experimentation.

Accordingly, the Applicant maintains that the specification fully enables the making and using of such rodents according to the pending claims without practicing undue experimentation.

The Applicant respectfully point out that in addition to standard methods of generating transgenic rodent, at the time the present application was filed methods of overcoming hurdles faced in generating transgenic rodents using standard techniques were also well known. For instance, the procedure of making transgenic rats was well known at the time the present application was filed (see Exhibit A: Reid et al., *Proc. Natl. Acad. Sci. USA*, 2001, 98(16):9271-6 and Exhibit B: Burkey et al., *J. Lipid Res.*, 1995, 36:1463-73). The Examiner has previously rejected the claims over the scope of the claims as covering "transgenic whales, transgenic fish [and] transgenic elephant" (Final Office Action dated May 18, 2006, page 4), and other animal species such as "cow, pig and sheep [as their] eggs are optically opaque, unlike mice" (Office Action dated August 30, 2005, page 9). The amended claims do not encompass of these animals cited by the Examiner. Further, the Examiner has not cited any reasoning as to why the claimed methods and compositions are not enabled as to specifically rodents. As non-mouse species of rodents are extremely identical to mouse species, both genetically and morphologically, the Examiner's reasoning as pertaining to whales, fish, elephants, cows, pigs and sheep should not apply to non-mouse rodents.

Accordingly, the Applicants maintain that once transgenesis is demonstrated in one rodent, as detailed in the present specification and described above, it is reasonable to conclude that the methods could be extrapolated to other rodents, in a similar manner without undue experimentation. Therefore, once the Applicants demonstrated the possibility of the described method with one rodent, it is reasonable to conclude that such methods can be used to generate other transgenic rodents using a vector that comprises a pair of P-element transposase recognized insertion sequences flanking an exogenous nucleic acid with a reasonable amount of experimentation.

Therefore, the Applicant asserts that the methods disclosed in the present specification in conjunction with the knowledge available in the art at the time the present application was filed, would enable one of ordinary skill in the art to practice the invention to the full scope of the claims.

In re Wands Factors

In addition to the above, as described in the Amendment and Response dated February 27, 2006, application of the *In re Wands* test to the facts of the present application must lead to the conclusion that the presently pending claims are fully enabled, as demonstrated below.

Under *In re Wands*, a determination of enablement requires consideration of eight factors, including: (a) the quantity of experimentation necessary; (b) the amount of direction or guidance presented; (c) the presence or absence of working examples; (d) the nature of the invention; (e) the state of the prior art; (f) the relative skill of those in the art; (g) the predictability or unpredictability of the art; and (h) the breadth of the claims.² Accordingly, under *In re Wands*, a determination of enablement is based on the combination of the factors, taken as a whole, not based solely on a single factor.

In the present application, the Applicant further maintains that the specification, coupled with the information known in the art, would enable one skilled in the art to use the invention without undue experimentation. However, in order to provide structure to the Applicant's response, each of the relevant enablement factors is further discussed in detail below.

(a) the unpredictability in the art and the quantity of experimentation necessary

The Applicant notes that the courts have clearly taught that the fact that experimentation may be complex does not necessarily make it undue, if the art typically engages in such experimentation. For example, see MPEP § 2164.01.³ Accordingly, the Applicant's citation of *Hybritech Inc. v. Monoclonal Antibodies, Inc.*, in the previous response was to emphasize that where the "experiments are empirical in nature," as in the case of the present application, the court found that no undue experimentation is required.⁴

In citing the research publications the Applicant have sought to establish that the field of generating transgenic rodents is not unpredictable. The publications cited herein represent only a small fraction of the total number of publications demonstrating the successful

2. *Ex Parte Forman*, 230 USPQ 546, 547 (Bd. Pat. App. & Interf. 1986); and, *In re Wands*, 8 USPQ2d 1400, 1404 (Fed. Cir. 1988).

3. See also *In re Certain Limited-Charge Cell Culture Microcarriers*, 221 USPQ 1165, 1174 (Int'l Trade Comm'n 1983), *aff'd sub nom.*, *Massachusetts Institute of Technology v. A.B. Fortia*, 227 USPQ 428 (Fed. Cir. 1985).

generation of transgenic rodents. Furthermore, the cited research publications establish that in order to make and use the transgenic rodent models according to the full scope of the claims in the present application, undue and excessive experimentation would not be required.

The methods disclosed in the cited reference used to generate the transgenic rodents were not exactly the same as the method disclosed in the present application. However, the publication has been cited to establish that by reporting the successful generation of rodent models, the cited publication have substantiated the Applicant's position that the field is not as unpredictable as asserted by the Examiner.

Therefore, since the field is not unpredictable, the fact that the experimentation may be complex does not necessarily make it undue, if the art typically engages in such experimentation, especially if the experimentation is empirical in nature. Accordingly, the Applicant maintains that the "how to make" and "how to use" requirements of 35 U.S.C. §112, first paragraph, have been fulfilled.

As such, the Applicant maintains that the art is replete with successful attempts at generating transgenic rodents. Therefore, the field cannot be as unpredictable and requiring of undue and excessive experimentation as the Examiner stresses. As such, the Applicant respectfully submits that the specification coupled with the information available in the art, at the time the application was filed, would enable one skilled in the art to use the invention without undue experimentation.

(b) the breadth of the claims and the amount of direction or guidance presented

The Applicant argues that the requirement for guidance in the specification shall be taken in conjunction with the guidance available in the art. As noted above, other methods of generating transgenic rodents are disclosed in the art. One skilled in the art of methods involving manipulating DNA and performing cell-based assays would be able to combine the guidance in the disclosure and the guidance available in the art to practice the claimed invention.

Accordingly, the Applicant maintains that the guidance provided in the specification and highlighted in the previous response, when taken in conjunction with the other enablement factors under *In re Wands*, provides the requisite amount of direction and guidance for a person skilled in the art to make and practice the invention to the full scope of the pending claims.

(c) the presence or absence of working examples

The Applicant respectfully notes that under the *In re Wands* factors for determining compliance with the enablement requirement under Title 35 U.S.C. §112, first paragraph, the presence or absence of working examples is but a single factor to be taken in consideration with the other factors. As such, under *In re Wands*, the presence or absence of working examples is weighed against the other factors, such as the availability in the art of general guidelines relevant to the claimed invention and guidance provided in the specification.

Moreover, the Applicant cites *In re Robbins* and *In re Borkowski* to emphasize that compliance with the enablement requirement under Title 35 U.S.C. §112, first paragraph does not require or mandate that a specific example be disclosed.⁵ Accordingly, the specification need not contain a working example if the invention is otherwise disclosed in such a manner that one skilled in the art would be able to practice the invention without undue experimentation.⁶

However, as the Examiner notes in the Office Action, the present application does contain working examples demonstrating the creation of transgenic mice using the P-element derived vectors. Therefore, the working examples, taken in conjunction with the general guidelines regarding creation of transgenic rodents available in the art and the guidelines disclosed in the specification, provides one skilled in the art adequate enablement to practice the claimed invention.

Accordingly, the Applicant maintains that the present application does enable a person skilled in the art, through the specification as well as the working example, sufficient

⁵ *In re Robbins* 166 U.S.P.Q. 552 (CCPA 1970); *In re Borkowski*, 164 U.S.P.Q. 642 (CCPA 1970).

⁶ *In re Borkowski*, 164 USPQ at 642.

enablement to apply the teachings in the specification in conjunction with the relevant art to make and use the claimed invention.

(d) the relative skill of those in the art

The Applicants maintain that the present invention involves methods of manipulating DNA and performing cell-based assays. As such, the Applicant notes that the skill level of an artisan, such as a laboratory technician or scientist with experience in molecular biology or the equivalent of a doctoral degree in molecular biology techniques, in using such methods is high.

In sum, the Applicant maintains that the enablement requirement has been met because a) the amount of experimentation required to create a transgenic rodent would not be undue and excessive b) working examples have been provided, c) guidance is given on how to generate and use such rodent models, and d) one of skill in the art would be able to perform the experiments as a matter of routine. The specification, therefore, provides sufficient enablement such that one of ordinary skill in the art would be able to practice the invention without undue experimentation.

As such, for at least the reasons described above, claims 11, 13-15, 18, 27, 30, 31 and 34 are adequately enabled by the specification. Accordingly, the Applicant respectfully requests the Examiner to withdraw this rejection of claims 11, 13-15, 18, 27, 30, 31 and 34 under 35 U.S.C. §112, first paragraph.

Claim Rejections – 35 U.S.C. § 112, second paragraph

Claims 11, 12, 16, 27 and 31 have been rejected under 35 U.S.C. § 112, second paragraph as allegedly being indefinite for failing to particularly point out and distinctly claim the subject matter which Applicant regards as the invention.

As claims 12 and 16 are canceled, the rejection of these claims is rendered moot.

Applicant has amended claim 11 by deleting the words "is inserted" in order to recite the language suggested by the Examiner. This amendment is to correct a grammatical error and does not change the scope of the claims.

Applicant has amended claims 27 and 31 by replacing “non-human and non-Drosophilidae animal . . . from said animal” with “rodent . . . from said rodent”. These claims as amended provide antecedent support for “said rodent”.

As amended claims 11, 27 and 31 are clear and definite, Applicant respectfully requests the Examiner to withdraw this rejection of these claims under 35 U.S.C. §112, second paragraph.


CONCLUSION

Applicant submits that all of the claims are in condition for allowance, which action is requested. If the Examiner finds that a telephone conference would expedite the prosecution of this application, please telephone the undersigned at the number provided.


The Commissioner is hereby authorized to charge any underpayment of fees associated with this communication, including any necessary fees for extensions of time, or credit any overpayment to Deposit Account No. 50-0815, order number TOSK-007CON.

Respectfully submitted,
BOZICEVIC, FIELD & FRANCIS LLP

Date: October 17, 2006

By: 
Robin C. Chiang, Ph.D.
Registration No. 46,619

Date: 10.17.06

By: 
Bret E. Field
Registration No. 37,620

Enclosure:

- Exhibit A: Reid et al., *Proc. Natl. Acad. Sci. USA*, 2001, 98(16):9271-6.
- Exhibit B: Burkey et al., *J. Lipid Res.*, 1995, 36:1463-73.

BOZICEVIC, FIELD & FRANCIS LLP
1900 University Avenue, Suite 200
East Palo Alto, California 94303
Telephone: (650) 327-3400
Facsimile: (650) 327-3231

An HIV-1 transgenic rat that develops HIV-related pathology and immunologic dysfunction

W. Reid^{*,†}, M. Sadowska[†], F. Denaro^{*}, S. Rao[‡], J. Foulke, Jr.[†], N. Hayes^{*}, O. Jones^{*}, D. Doodnauth^{*}, H. Davis^{*}, A. Sill[§], P. O'Driscoll[§], D. Huso[¶], T. Fouts[¶], G. Lewis^{||**}, M. Hill^{||}, R. Kamin-Lewis^{||**}, C. Wei^{††}, P. Ray^{‡‡}, R. C. Gallo[†], M. Reitz^{†**}, and J. Bryant^{**§§}

^{*}Animal Model Division and Divisions of [†]Basic Science, [‡]Vaccine Research, and [§]Epidemiology and Prevention, Institute of Human Virology, University of Maryland, Baltimore, MD 21201; [¶]Division of Comparative Medicine and ^{**}Department of Microbiology and Immunology, University of Maryland, Baltimore, MD 21201; ^{††}Division of Thoracic and Cardiovascular Surgery, School of Medicine, University of Maryland, Baltimore, MD 21201; ^{‡‡}Children's Research Institute, Children's National Medical Center, Washington, DC 20010; and ^{||}Division of Comparative Medicine, Johns Hopkins University School of Medicine, Baltimore, MD 21205

Contributed by R. C. Gallo, June 11, 2001

We report, to our knowledge, the first HIV type 1 (HIV-1) transgenic (Tg) rat. Expression of the transgene, consisting of an HIV-1 provirus with a functional deletion of *gag* and *pol*, is regulated by the viral long terminal repeat. Spliced and unspliced viral transcripts were expressed in lymph nodes, thymus, liver, kidney, and spleen, suggesting that Tat and Rev are functional. Viral proteins were identified in spleen tissue sections by immunohistochemistry and gp120 was present in splenic macrophages, T and B cells, and in serum. Clinical signs included wasting, mild to severe skin lesions, opaque cataracts, neurological signs, and respiratory difficulty. Histopathology included a selective loss of splenocytes within the periarterial lymphoid sheath, increased apoptosis of endothelial cells and splenocytes, follicular hyperplasia of the spleen, lymphocyte depletion of mesenteric lymph nodes, interstitial pneumonia, psoriatic skin lesions, and neurological, cardiac, and renal pathologies. Immunologically, delayed-type hypersensitivity response to keyhole limpet hemocyanin was diminished. By contrast, Ab titers and proliferative response to recall antigen (keyhole limpet hemocyanin) were normal. The HIV-1 Tg rat thus has many similarities to humans infected with HIV-1 in expression of viral genes, immune-response alterations, and pathologies resulting from infection. The HIV-1 Tg rat may provide a valuable model for some of the pathogenic manifestations of chronic HIV-1 diseases and could be useful in testing therapeutic regimens targeted to stages of viral replication subsequent to proviral integration.

HIV type 1 (HIV-1) infection is marked by a constellation of pathologies in addition to a variety of secondary infections (1). These include central and peripheral neuropathies (2), follicular lymph node hyperplasia (particularly early in infection; ref. 3), lymphoid depletion (at least in part involving apoptosis; refs. 4 and 5), interstitial pneumonitis (especially in pediatric cases; refs. 6 and 7), tubulointerstitial nephritis, glomerulosclerosis (8–10), wasting (11), and heart disease (12).

To establish a small-animal model for HIV-associated pathologies, several HIV transgenic (Tg) mice have been established. A *Tat* transgene was reported to cause dermal lesions resembling Kaposi sarcoma (13) or lymphoid hyperplasia in spleen and lymph nodes, and B cell lymphoma (14) when expression was regulated by the viral long terminal repeat (LTR) or a heterologous promoter, respectively. Expression of a *nef* transgene driven by the HIV-1 LTR also resulted in dermal lesions (15). More recently, Tg mice expressing *nef* under the control of a human T cell-specific promoter and mouse enhancer developed immunodeficiency with loss of T cells and alterations of T cell function (16). Tg mice also have been constructed with a *gag-pol*-deleted HIV-1 provirus regulated by the viral promoter and are characterized by wasting/runting, psoriatic skin lesions, cataracts, and nephropathy. Some HIV-1 gene expression occurs in most tissues, but is highest in skin and muscle (17, 18).

Despite replicating some of the pathologies in humans, viral expression in many existent HIV-1 Tg mouse models is regulated either by heterologous promoters, resulting in expression in atypical tissues, or by the viral promoter, which gives the highest expression in skin. The viral promoter does not function normally in mice, in part because mouse cyclin T does not interact functionally with Tat (19). We report here the construction of Tg rats that contain a *gag-pol*-deleted HIV-1 provirus regulated by the viral promoter. Unlike mice with the same transgene, efficient viral gene expression occurs in lymph nodes, spleen, thymus, and blood, suggesting a functional Tat. The Tg rat thus may offer significant advantages as a noninfectious small-animal model of HIV-1 pathogenesis.

Materials and Methods

Construction of HIV-1 *gag-pol*-Tg Rat. The construction of the plasmid from which the transgene was derived has been described (17). Briefly, a 3-kbp *SphI*-*MscI* fragment encompassing the 3' region of *gag* and the 5' region of *pol* was removed from pNL4-3, an infectious proviral plasmid, to make the noninfectious HIV-1 *gag-pol* clone pEVd1443. A 7.4-kbp *EaeI*-*NaeI* fragment containing the provirus and host cell flanking regions was microinjected into fertilized one-cell Sprague-Dawley × Fisher 344/NHsd F1 eggs as described (20). The experimental protocol was approved by the University of Maryland Biotechnology Institute Institutional Animal Care and Use Committee.

Macrophages and B and T Cell Isolation. Splenocytes were purified on Histopaque-1083 (Sigma), counted, divided into 3 aliquots of 1.5×10^7 cells, and stained with primary mAbs by standard procedure (21). Each aliquot was labeled for 45 min at room temperature with a 1:100 dilution of anti-rat mAbs ED1 (MCA341R; Serotec), CD45RA (MCA340R; Serotec), or CD3 (22011D; PharMingen), which are specific for rat macrophages and B and T cells, respectively. Cells (10^6) were magnetically labeled with 20 μ l of magnetic activated cell sorting (MACS) rat anti-mouse IgG1 (471-02) or goat anti-mouse IgG (484-02) (Miltenyi Biotec, Auburn, CA) for 15 min at 6–12°C. The magnetically labeled cell suspensions were separated by positive selection on MS+ separation columns placed in a VarioMACS magnet (Miltenyi Biotec), using the manufacturer's recommendations.

Abbreviations: DTH, delayed type hypersensitivity; H&E, hematoxylin and eosin; HIV-1, HIV type 1; KLH, keyhole limpet hemocyanin; PALS, periarterial lymphatic sheath; Tg, transgenic; LTR, long terminal repeat; Th, T helper.

^{§§}To whom reprint requests should be addressed at: Animal Model Division, Institute of Human Virology, 725 West Lombard Street, Baltimore, MD 21201-1192. E-mail: bryant@umbi.umd.edu.

The publication costs of this article were defrayed in part by page charge payment. This article must therefore be hereby marked "advertisement" in accordance with 16 U.S.C. §1734 solely to indicate this fact.

Histology, Immunocytochemistry, and Apoptosis. Tissues from Tg and non-Tg littermates and Fisher 344/NHsd Sprague–Dawley control rats were fixed in 10% neutral buffered formalin and embedded in paraffin. Five-microgram tissue sections were used for hematoxylin and eosin (H&E) staining, immunohistochemistry, and apoptosis assays. A modified avidin/biotin method was used for immunohistochemical localization of HIV gene products (22). Paraffin sections were processed as described, exposed to antigen unmasking solution (Vector Laboratories), incubated in 3% H₂O₂ for 20 min, and treated with avidin/biotin blocking solution (Vector Laboratories) and nonimmune sera appropriate for blocking the secondary Ab at a 1:5 dilution. Primary Abs (all from Advanced Biotechnologies, Columbia, MD, except where noted) included HIV-1 gp120 goat antiserum (13-202-000), diluted 1:50 and 1:100; HIV-1 rabbit anti-HIV gp120 antiserum (13-204-000), diluted 1:100; mouse anti-HIV-1 gp120 mAb (NEN, Boston, MA; NEA 9301), diluted 1:150; mouse anti-HIV-1 Tat mAb (13-162-100), diluted 1:50 and 1:100; and mouse anti-HIV-1 Nef (13-152-1000), diluted 1:50 and 1:100. Biotinylated secondary Abs were incubated for 2 h at room temperature with anti-mouse IgG (rat-absorbed), anti-rabbit IgG, and anti-goat IgG (Vector Laboratories), at dilutions of 1:200–500, and labeled with Vecta Stain Elite ABC kit (Vector Laboratories), followed by addition of 3,3'-diaminobenzidine tetrahydrochloride (DAB) peroxidase (Sigma) or the 3-amino-9-ethylcarbazole (AEC) substrate system (Dako) to visualize the immunolabel.

Immunization of Rats. Tg and Fisher 344/NHsd control rats were immunized i.p. with 100 μ g of keyhole limpet hemocyanin (KLH; Pierce) with complete Freund's adjuvant (Difco). Four weeks later, sera were collected, and anti-KLH end-point titers were determined by ELISA. Microtiter plates (NUNC Maxi-Sorp, Roskilde, Denmark) were coated with 2 μ g/ml KLH overnight at 4°C. Plates were washed, blocked with 5% milk powder, and incubated with serially diluted rat sera at 37°C for 2 h. Bound IgG was detected with horseradish peroxidase-conjugated anti-rat IgG Ab. For detection of delayed type hypersensitivity (DTH), rats were challenged intracutaneously 4 weeks after immunization with 50 μ g of KLH, and the size of the induration was measured 24 h later.

Proliferation Assays. Splenocytes (2.0×10^5) were cultured in 0.2 ml of RPMI medium 1640 with 10% (vol/vol) FBS in a microtiter plate with 50 μ g/ml of KLH or 10 μ g/ml of phytohemagglutinin. The cells were pulsed with 1 μ Ci of [³H]thymidine (6.7 Ci/mmol; NEN) for 18–24 h and harvested onto glass fiber filters with a Micron 96-cell harvester (Skatron, Lier, Norway). Incorporation of [³H]thymidine was measured with a liquid scintillation counter. All experiments were in triplicate.

Statistics. The mean number of apoptotic splenocytes per high power field, DTH measurements, and KLH end-point titers between phytohemagglutinin-stimulated and unstimulated cells from Tg and normal offspring were compared by using an independent Student's *t* test for samples exhibiting normally distributed values. A Wilcoxon rank sum test was used for samples exhibiting non-normal distribution. Two-tailed *P* values were considered significant at *P* < 0.05.

Results

Preliminary Analysis of HIV-1 Tg Rats. One female founder was produced that had very opaque cataracts. Mating with a wild-type Fischer 344/NHsd produced several F1 Tg and normal offspring. F1 offspring had very opaque (line 1) or very mild cataracts (line 2). The Tg animals were grouped according to cataract phenotypes, and DNA was prepared from tail tips, digested with *Eco*RI, and analyzed by Southern blotting (ref. 23;

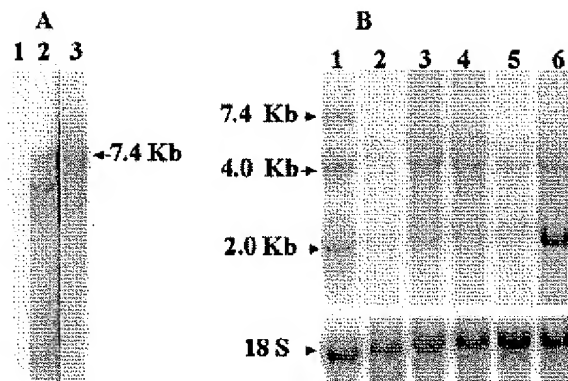


Fig. 1. Detection and expression of transgene. (A) Detection of transgene. A Southern blot was performed on *Eco*RI-digested DNA from tail snips of a normal rat (15 μ g; lane 1) or Tg rats with mild (20 μ g; lane 2) or very opaque (5 μ g; lane 3) cataracts. The blot was hybridized to an α -³²P-labeled 7.4-kb *Eae*I–*Nae*I fragment from pEvd1443. (B) Expression of transgene RNA. A Northern blot was performed on total RNA isolate from various tissues and analyzed by Northern blot as described (32). HIV-specific transcripts (7-, 4-, and 2-kb) were detected with an α -³²P-labeled 1.3-kbp (*Bgl*II/*Bgl*II) fragment from pHX82, containing gp41 and *nef* coding regions. HIV transcripts were quantified with a Storm 840 PhosphorImager (Molecular Dynamics) and normalized for hybridization to 18S rRNA by using an appropriate probe. RNA was from the axillary (lane 1) and mesenteric (lane 2) lymph nodes, thymus (lane 3), liver (lane 4), kidney (lane 5), and spleen (lane 6) of transgenic rat with highly opaque cataracts. The positions of the 7.0-kb full-length mRNA, 4-kb singly spliced *env* mRNA, and 2-kb multiply spliced mRNA are indicated.

Fig. 1A). *Eco*RI cuts the transgene once. As shown in lanes 2 and 3 of Fig. 1A, the hybridization patterns of DNA representing the two phenotypes differed. Both gave bands corresponding to a full-length transgene, as indicated by the arrow, suggesting that both integration sites contained two or more tandem copies of the transgene. Other bands, presumably representing transgene–host junction bands or head-to-tail multiple tandem integrated transgenes, differed, suggesting that the transgene had integrated at two independently segregating sites, one resulting in the opaque cataract phenotype and the other in mild cataracts. A brother–sister mating of F1 Tg rats from line 2 produced offspring with mild cataracts only. Southern blots of *Eco*RI-digested DNA from offspring were identical to those of the parents. As judged by the relative intensity of hybridization to Southern blots of Tg DNA compared with serial dilutions of known amounts of plasmid DNA quantified with a PhosphorImager (Molecular Dynamics), Tg rats from line 1 contained 20–25 copies, whereas those of line 2 contained only a few. Subsequent studies focused only on line 1 HIV-1 Tg rats.

HIV-1 Transgene Expression. RNA from numerous tissues was analyzed for viral transcripts. Expression levels were generally highest in lymph nodes, spleen, kidney, and thymus. A representative Northern blot of lymph node RNA (Fig. 1B) shows three viral-specific bands, representing full-length 7.4-kb mRNA, 4.0-kb singly spliced *Env* mRNA, and multiply spliced 2-kb mRNA transcripts for *Nef*, *Tat*, and *Rev*. The presence of *Tat* mRNA in the 2-kb band from spleen RNA was confirmed by reverse transcription–PCR amplification and DNA sequence analysis (not shown). Formalin-fixed paraffin-embedded 5- μ m sections of spleen from line 1 (Fig. 1B) Tg rats were analyzed by immunohistochemistry for *Env* gp120, *Nef*, and *Tat*. All three proteins were evident in cells within the red and white pulp of the spleen (Fig. 2A–C). Gp120 was present in cellular lysates of spleen-derived macrophages and B and T cells as judged by

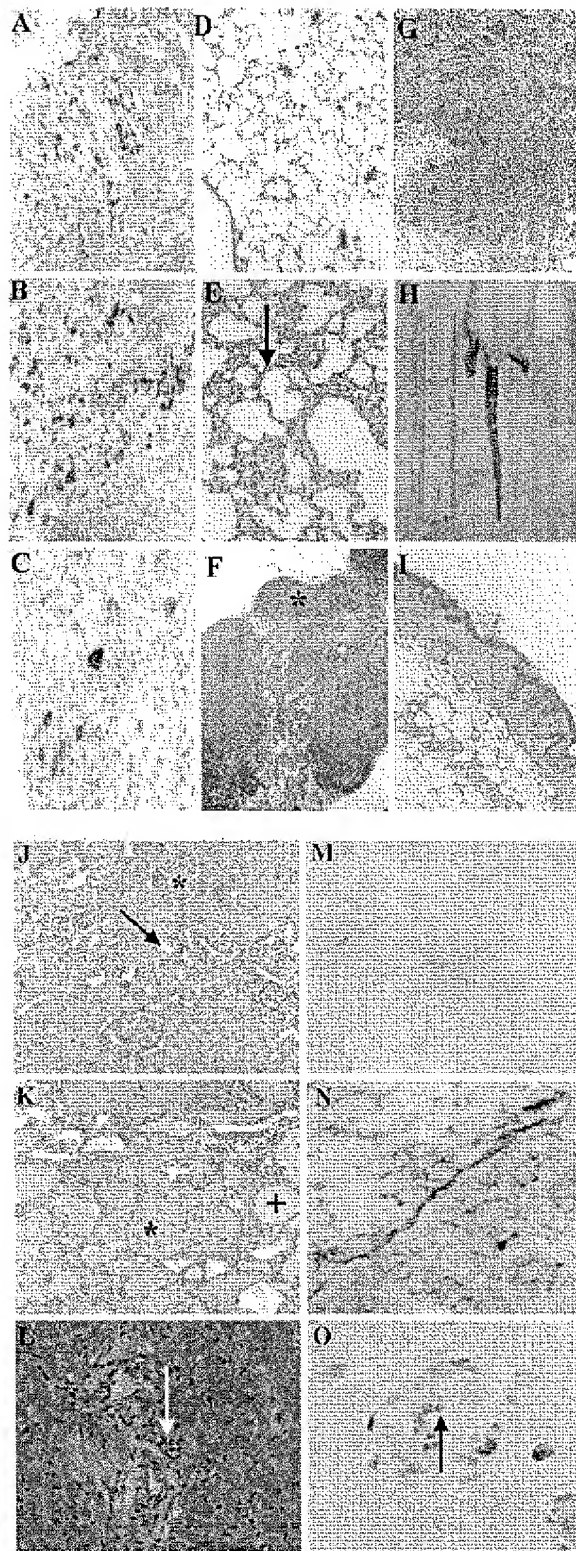


Fig. 2. Pathology and transgene expression. A section of Tg rat spleen was stained for HIV gp120 (A), Nef (B), and Tat (C). Cytoplasmic staining (dark brown) is evident for all three proteins (original magnification = $\times 50$). H&E-stained sections of control (D) and Tg (E) lung are shown ($\times 20$). Arrow in

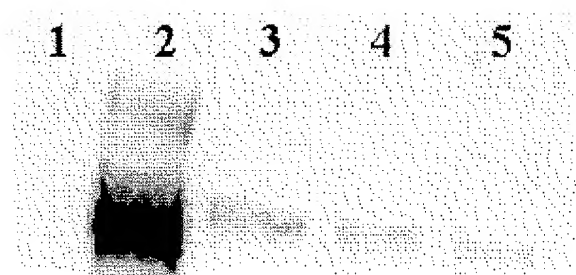


Fig. 3. Transgene expression in splenocytes. Seven micrograms of protein from extracts of spleen-derived macrophages (lane 3), B cells (lane 4), or T cells (lane 5) was fractionated on a 4–12% NuPage gel (NOVEX, San Diego) and analyzed by Western blot, using a 1:100 mouse anti-HIV-1 gp120 mAb (NEA 9301, NEN). Proteins were visualized by using the enhanced chemiluminescence (ECL) plus Western blotting system (Amersham Pharmacia). Lane 1 contained extract from a normal control spleen, and lane 2 contained 30 ng of recombinant gp120 as a positive control.

Western blotting (Fig. 3). The animals were also antigenemic. As measured by ELISA, sera contained 100–200 pg/ml of gp120 (Table 1). Thus, in marked contrast to Tg mice with the same proviral transgene (17, 18), Tg rats express viral gp120 in macrophages and B and T cells and shed it into peripheral blood.

Pathology of Tg Rats. Cataract formation ranged from mild to highly opaque. Some Tg animals ($>50\%$) presented with highly angiogenic corneas. Their lenses had marked vacuolization, liquefaction, and fragmentation (not shown). In addition to cataracts, HIV-1 Tg rats developed many clinical manifestations of AIDS by 5–9 months of age, including weight loss, neurological abnormalities, and respiratory difficulty. Generally, neurological abnormalities were characterized by circling behavior and hind-limb paralysis. Often ($>70\%$), the lung showed mild interstitial fibrosis and mononuclear cell infiltration (Fig. 2 D and E). Mesenteric lymph nodes ($>40\%$) were generally enlarged, and many histological sections showed lymphoid depletion and fibrosis (Fig. 2 F and G). Many Tg rats ($>20\%$) had focal to extensive ulcerative skin lesions (Fig. 2 H and I). Histologically, the lesions were hyperkeratotic, with elongation of the rete ridges. The kidneys from clinically ill rats ($>90\%$) were diffusely pale, and the capsular surface was pitted, similar to what is seen with HIV-1 associated-nephropathy. H&E-stained kidney sections showed a spectrum of renal disease varying from mild to severe. Generally, glomeruli in Tg rats contained increased periodic acid/Schiff reagent (PAS)-positive material, with either segmental or global sclerosis. Some glomeruli showed mesangial hypercellularity and enlargement of visceral epithelial cells. Silver staining confirmed that the PAS-positive tissue within the

E indicates area of interstitial thickening. H&E-stained sections of control (F) and Tg (G) mesenteric lymph node ($\times 10$) are shown. Note normal follicle (*), F and hemorrhage, lymphoid depletion, and vascular proliferation in Tg section (G). Gross tail and foot lesions (H) and H&E-stained Tg skin ($\times 60$). Note psoriatic skin lesions with hyperkeratosis and mononuclear cell infiltrate (arrow, I). H&E-stained control kidney shows normal glomerulus (*) and renal tubule (arrow, J); Tg kidney shows focal glomerulosclerosis (*) and tubulointerstitial disease (+, K; $\times 60$). H&E-stained heart section (L) shows myocardial inflammation with mononuclear cell infiltration (arrow) ($\times 60$). Astrocytes from normal (M) or Tg (N) brains were stained for glial fibrillary acidic protein (GFAP; $\times 40$). Staining for GFAP was as reported (22), using anti-GFAP Ab (U7038; Dako). Staining of normal brain was limited, but Tg brain was heavily stained, indicating reactive gliosis, a marker for central nervous system damage. (O) Blood vessels in Tg brain were stained with ApoptTag ($\times 60$); arrow indicates vascular endothelial apoptosis.

Table 1. Serum gp120 in Tg rats

Tg rats	gp120, pg/ml*
Tg no. 1	151
Tg no. 2	129
Tg no. 3	121
Tg no. 4	85
Tg no. 5	172
Tg no. 7	235
Tg no. 8	164
Tg no. 9	217

The expression of gp120 envelope protein in the serum was assayed by ELISA antigen capture assay. The average gp120 concentration in the serum of hemizygous rats ($n = 9$) was 141 pg/ml (A).

*Capture ELISAs were done in triplicate on Tg rats with negative controls ($n = 8$). A mean adjusted value (76.6) for negative controls was subtracted.

glomeruli was composed of matrix material (not shown). The renal tubules showed microcystic tubular and tubulointerstitial pathology characterized by tubular degeneration, interstitial fibrosis, and mononuclear cell infiltration (Fig. 2J and K). The heart generally was round and pale in color (not shown). Some hearts from Tg rats showed evidence of endocarditis and myocardial inflammation characterized by necrosis, mononuclear cell infiltrates, and multiple vascular abnormalities (Fig. 2L).

Tg rat brains with or without clinical neurological signs were grossly unremarkable. However, pathologic changes were evident in rats with clinical signs. Capillaries and endothelial cells presented with atypical changes, such as microscopic hemorrhages and endothelial cell apoptosis, in a multifocal distribution (Fig. 2O). Foci of gliosis together with neuronal cell death were noted, particularly in animals with clinically observable signs (Fig. 2N). For comparison, Fig. 2M shows a normal section of brain. Although the distribution of these changes seemed random, when they occurred with increased severity in focal areas of the brain, corresponding neurological deficits were noted. For example, animals with motor problems presented with greater severity of changes in the caudate putamen and substantia nigra.

Tg rat spleen was generally normal in size. Spleen tissue sections showed a loss of splenocytes within the periarterial lymphatic sheath (PALS), expansion of the marginal zones, follicular hyperplasia, and apoptosis of endothelial cells and splenocytes (Fig. 4A and B). Apoptosis of splenocytes was evaluated by counting ApopTag (Intergen, Purchase NY)-positive cells per high-powered field in 5-month-old male rats and was significantly elevated compared with age- and sex-matched non-Tg controls ($P < 0.01$; Fig. 4C).

Immune Function of HIV-1 Tg Rats. To evaluate immune function, Tg rats and age-matched controls were immunized with KLH, and the resultant KLH-specific DTH responses and anti-KLH Ab titers were determined. The DTH response was determined from the extent of induration present at 24 h. The induration was significantly lower relative to controls ($P < 0.01$; Table 2). In contrast, there was no significant difference in anti-KLH-specific Ab titers, suggesting that the Tg rats have an abnormal T helper (Th)-1 response but normal Th2 function. The mean proliferative response of spleen cells from adult Tg rats to nonspecific mitogen (phytohemagglutinin) was significantly increased after 6 days compared with littermate controls ($P = 0.0062$; Table 3). However, there were no statistical differences in the T cell proliferative response of splenocytes from vaccinated rats to a recall antigen (KLH).

Discussion

We report, to our knowledge, the first HIV-1 Tg rat. The transgene, consisting of an HIV-1 provirus deleted for *gag* and

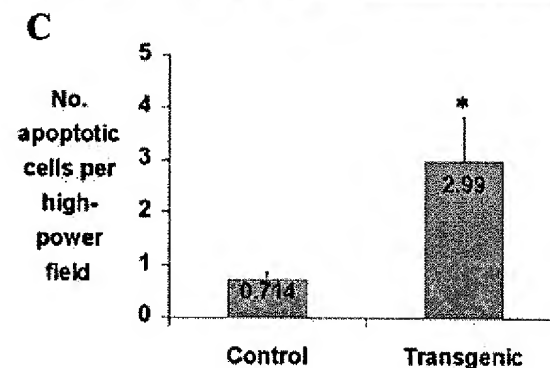
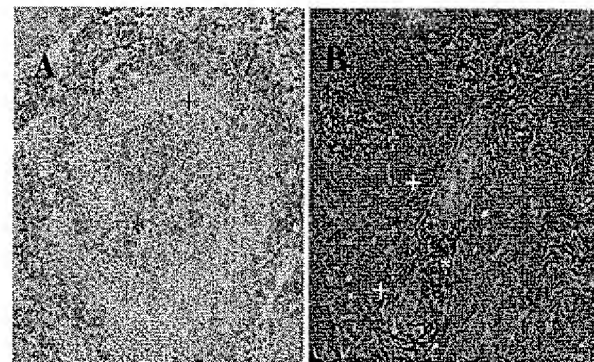


Fig. 4. Pathology and apoptosis in Tg rat spleen. (A) H&E-stained control spleen. Note T cell region (PALS) (*) and B cell region (marginal zone) (+) (original magnification $\times 60$). (B) H&E-stained Tg rat spleen ($\times 60$). Note loss of T cells within the PALS (*). The two + show the marginal zone. (C) Five-micrometer tissue sections were assayed *in situ* for apoptosis by using an ApopTag kit. Spleen sections from 5-month-old male Tg and Fisher 344/NHsd control rats were taken from 3 animals per group, and apoptotic cells from each section were enumerated 3 times at $\times 400$ by using a Nikon Labophot-2 light microscope. The entire tissue section was counted by using a stage micrometer to pick successive nonoverlapping fields. The * shows the statistically significant difference between HIV-1 transgenic rats and age-matched controls.

pol, is expressed in lymphoid tissues, including lymph nodes, spleen, thymus, and blood. The Tg rats exhibit pathologies and immune irregularities characteristic of HIV-1 infection of humans.

The tissue-specific pattern of viral gene expression is of interest. To model viral gene expression in infected humans, we

Table 2. Antibody and DTH responses to KLH in HIV-1 Tg rats

Exp. group	Observations	Anti-KLH Ab titer	Anti-KLH DTH, mm diameter	SE
Tg*	12	7.4	NA	0.19
Control*	6	7.9	NA	0
Tg†	10	NA	3.5†	0.7
Control†	6	NA	10.8	1.4

NA, not applicable.

*Tg and non-Tg rats were immunized i.p. with 100 μ g of KLH with complete Freund's adjuvant. Four weeks later, sera was collected, and end-point anti-KLH Ab titers were determined by ELISA. The results are expressed as mean \pm SE (logarithm 10) of end-point titers.

†Immunized rats were challenged with 50 μ g of KLH intracutaneously, and the size of the induration was measured 24 h later. Results are expressed as mean \pm SE of diameter of induration (mm).

‡Indicates a statistical significance between HIV-1 Tg and non-Tg rats.

Table 3. Proliferative response of splenocytes from Tg

Exp. group	Observations	[³ H]thymidine incorporation of stimulated spleen cells, Δcpm		
		PHA	KLH	SE
Tg*	8	28,289 [†]	NA	7,201
Control*	5	2,138	NA	1,070
Tg [†]	4	NA	89,202	18,147
Control [†]	3	NA	92,475	24,260

NA, not applicable.

*Spleen cells (2×10^5) from HIV-1 Tg or non-Tg rats were cultured with 10 μ g/ml of PHA at 37°C for 6 days.

[†]Spleen cells (2×10^5) from HIV-1 Tg or non-Tg rats immunized with KLH 4 weeks previously were cultured with 50 μ g/ml KLH at 37°C for 5 days. All cells were labeled with 1 μ Ci [³H]thymidine for the last 18–24 h, harvested, and the incorporated radioactivity counted. The results are expressed as mean \pm SE of thymidine incorporation in triplicate cultures.

[†]Indicates a statistical significance between Tg and non-Tg rats.

used the viral LTR to regulate the transgene. LTR-regulated gene expression depends on transactivation by the viral Tat protein, which requires cellular cyclin T as a cofactor. Mouse cyclin T is not functional with Tat, and LTR-driven expression in Tg mice differs from expression in humans, with the highest levels in skin and muscle. In contrast, viral genes are efficiently expressed in lymphoid tissues of Tg rats, similar to infected humans, suggesting that rat cyclin T is functional. A similar suggestion has been made by Bieniasz and Cullen (24). Three sizes of viral transcripts can be detected, including a 7.4-kb unspliced mRNA, a 4.3-kb singly spliced (*env*) mRNA, and a 2-kb multiply spliced (*tat*, *rev*, and *nef*) mRNA, similar to infected human cells, suggesting that Rev, a viral protein that regulates splicing, can also function in rats.

Clinical manifestations, similar to those in humans infected with HIV, are evident in the Tg rats, including neurological changes, respiratory difficulty, and cataracts. The neuropathology includes reactive gliosis, neuronal cell loss, lymphocyte infiltration, and alteration of endothelial cells with loss of blood–brain barrier integrity. There is a degeneration of peripheral nerves and skeletal muscle atrophy similar to that in infected humans. The Tg rat could be a useful model of HIV–central nervous system interactions, because the neuroanatomy, neurophysiology, neuropathology, and behavior of rats are well studied.

Pneumonitis associated with HIV-1 infection is common in pediatric cases of AIDS (6); however, its pathogenesis is not well understood. Most cases of pneumonia in people infected with HIV-1 are characterized by lymphocytic interstitial pneumonitis. Respiratory difficulty in the Tg rats is correlated with a mild expansion of the lung interstitium by a mononuclear infiltrate. The pneumonia in the Tg rats is unlikely to be caused by opportunistic infections, because of their pathogen-free status,

sterile housing conditions, and certified diet, suggesting that pathogenesis is mediated directly by the HIV-1 transgene.

Cardiac disorders including myocarditis and cardiomyopathies have been reported in patients infected with HIV, but their etiopathogenesis is uncertain (12, 25, 26). The cardiac pathology seen in the Tg rats is grossly and microscopically similar to that in infected people, suggesting that this could be a useful model for the study of HIV-associated cardiac disease. There is controversy about the role of HIV as the primary etiology of cardiac pathology; opportunistic infections, cardiotoxic substances, nutritional deficiencies, and autoimmune reactions have been suggested as contributing factors. Because the Tg rats are pathogen-free, the observed cardiac abnormalities are likely caused by viral gene product activity rather than opportunistic infections.

Renal abnormalities are frequently seen in AIDS, especially in African-American patients (8, 27, 28). The most typical is HIV-1 associated-nephropathy (HIVAN), occurring in 10–15% of all infected African-American patients. HIVAN includes proteinuria, nephrotic syndrome, focal or segmental glomerulosclerosis, and tubulo-interstitial disease, rapidly progressing to end-stage renal disease. The pathogenesis is not completely understood but likely involves the direct effects of HIV-1 and cytokines such as basic fibroblast growth factor (bFGF) and transforming growth factor (TGF)- β (28) that are secreted by infected cells (29). The Tg rat offers a potential model for HIVAN and related conditions.

HIV-1 Tg rats have selective immune abnormalities. There is a markedly decreased DTH response but Ab titers and the proliferative response of splenocytes to KLH antigen is normal. Lymphoid tissues manifest an AIDS-like histopathology, including lymphocyte depletion in lymph nodes, severe splenic hyperplasia with loss of cells around the PALS, and increased apoptosis of splenocytes. Viral proteins are expressed in spleen T and B cells and monocytes. This hyperplasia and cell loss may be caused in part by abnormal trafficking of cells or by abnormal or selective proliferation and loss of lymphocyte subsets. It has recently been shown in mice that CD8 α^+ dendritic cells and naïve and Th1 T cells concentrate within the PALS, whereas CD8 α^+ dendritic cells and Th2 cells form loose rings around the outer PALS in close proximity to the B cells (30, 31). It is tempting to speculate that the loss of T cells around the PALS and in lymph nodes, the increased apoptosis in spleen, and the diminished DTH reaction are the results of a common mechanism affecting Th1 development or trafficking. Taken together with the pattern of pathologies that occur, the HIV-1 Tg rat is potentially a highly useful small-animal model for AIDS pathogenesis.

We thank the Institute of Human Virology ELISA Core Facility, Manhattan Charurat, Sayhed Abdel-Wahab, and Drs. David Hone, Simon Agwale, and Minglin Li for supporting this study. This research was supported in part by Public Health Service Grants 1K08 AI01792, NS 31857, and NS 39250, and by the Elisabeth Glaser Grant for Studies in Pediatric AIDS.

- Popovic, M. & Gartner, S. (1989) *Curr. Opin. Immunol.* 1, 516–520.
- Price, R. W. (1996) *Lancet* 348, 445–452.
- Burke, A. P., Benson, W., Ribas, J. L., Anderson, D., Chu, W. S., Smialek, J. & Virmani, R. (1993) *Am. J. Pathol.* 142, 1701–1713.
- Gallo, R. C. & Montagnier, L. (1988) *Sci. Am.* 259, 41–48.
- Fauci, A. S. (1993) *Eur. J. Immunol.* 23, 1011–1018.
- McSherry, G. D., Mootsikapun, P., Chetchotisakd, P., Intarapoka, B., Schneider, R. F. & Rosen, M. J. (1996) *Semin. Respir. Infect.* 11, 173–183.
- Mootsikapun, P., Chetchotisakd, P. & Intarapoka, B. (1996) *J. Med. Assoc. Thai* 79, 477–485.
- Bourgoignie, J. J., Glascock, R. J., Cohen, A. H., Danovitch, G. & Parsa, K. P. (1989) *Klin. Wochenschr.* 67, 889–894.
- Seney, F. D., Jr., Burns, D. K., Silva, F. G., Bourgoignie, J. J., Glascock, R. J., Cohen, A. H., Danovitch, G. & Parsa, K. P. (1990) *Am. J. Kidney Dis.* 16, 1–13.
- Klotman, P. E. (1999) *Kidney Int.* 56, 1161–1176.

- Strawford, A. & Hellerstein, M. (1998) *Semin. Oncol.* 25, 76–81.
- Patel, R. C. & Frishman, W. H. (1996) *Med. Clin. N. Am.* 80, 1493–1512.
- Vogel, J., Hinrichs, S. H., Reynolds, R. K., Luciw, P. A. & Jay, G. (1988) *Nature (London)* 335, 606–611.
- Vellutini, C., Horschowski, N., Philippon, V., Gambarelli, D., Nave, K. A. & Filippi, P. (1995) *AIDS Res. Hum. Retroviruses* 11, 21–29.
- Dickie, P., Ramsdell, F., Notkins, A. L. & Venkatesan, S. (1993) *Virology* 197, 431–438.
- Hanna, Z., Kay, D. G., Rebai, N., Guimond, A., Jothy, S. & Jolicœur, P. (1998) *Cell* 95, 163–175.
- Dickie, P., Felser, J., Eckhaus, M., Bryant, J., Silver, J., Marinos, N. & Notkins, A. L. (1991) *Virology* 185, 109–119.
- Santoro, T. J., Bryant, J. L., Pellicoro, J., Klotman, M. E., Kopp, J. B., Bruggeman, L. A., Franks, R. R., Notkins, A. L. & Klotman, P. E. (1994) *Virology* 201, 147–151.

19. Wei, P., Garber, M. E., Fang, S. M., Fischer, W. H. & Jones, K. A. (1998) *Cell* **92**, 451–462.
20. Lacy, E., Costantini, F., Beddington, R. & Hogan, B., eds. (1994) *Manipulating the Mouse Embryo* (Cold Spring Harbor Lab. Press, Plainview, NY).
21. Coligan, J. E., Kruisbeek, A. M., Margulies, D. H., Shevach, E. M. & Strober, W., eds. (1994) *Current Protocols in Immunology* (Wiley, New York).
22. Wiley, C. A., Schrier, R. D., Denaro, F. J., Nelson, J. A., Lampert, P. W. & Oldstone, M. B. (1986) *J. Neuropathol. Exp. Neurol.* **45**, 127–139.
23. Southern, E. M. (1975) *J. Mol. Biol.* **98**, 503–517.
24. Bieniasz, P. D. & Cullen, B. R. (2000) *J. Virol.* **74**, 9868–9877.
25. Barbaro, G., Di Lorenzo, G., Grisorio, B. & Barbarini, G. (1998) *AIDS Res. Hum. Retroviruses* **14**, 1071–1077.
26. Guillaumon, T. L., Romeu, F. J., Porcada Sainz, J. M., Curos, A. A., Larrousse, P. E. & Valle, T. V. (1997) *Rev. Esp. Cardiol.* **50**, 721–728.
27. Bourgoignie, J. J., Ortiz-Interian, C., Green, D. F. & Roth, D. (1989) *Transplant. Proc.* **21**, 3899–3901.
28. Ray, P. E., Liu, X. H., Xu, L. & Rakusan, T. (1999) *Pediatr. Nephrol.* **13**, 586–593.
29. Liu, X. H., Hadley, T. J., Xu, L., Peiper, S. C. & Ray, P. E. (1999) *Kidney Int.* **55**, 1491–1500.
30. Randolph, D. A., Huang, G., Carruthers, C. J., Bromley, L. E. & Chaplin, D. D. (1999) *Eur. J. Immunol.* **28**, 2159–2162.
31. Moser, M. & Murphy, K. M. (2000) *Nat. Immunol.* **1**, 199–205.
32. Puissant, C. & Houdebine, L. M. (1990) *BioTechniques* **8**, 148–149.

Overexpression of human apolipoprotein A-I in transgenic rats and the hyperlipoproteinemia associated with experimental nephrosis

Bryan F. Burkley,^{1,*} Dennis France,^{*} Hongxing Wang,[†] Xiaowen Ma,^{*} Barbara Brand,^{*} Colleen Abuhani,^{*} Margaret R. Diffenderfer,[†] Julian B. Marsh,[†] James R. Paterniti, Jr.,^{*} and Edward A. Fisher^{1,†}

Department of Metabolic Diseases,^{*} Preclinical Research, Sandoz Research Institute, Sandoz Pharmaceuticals Corporation, East Hanover, NJ 07936, and Biochemistry Department,[†] Medical College of Pennsylvania, Philadelphia, PA 19129

Abstract Hyperlipoproteinemia contributes both to kidney disease progression and the development of atherosclerosis. Elevated high density lipoprotein cholesterol and apolipoprotein A-I (apoA-I) serum levels are independent factors protective against the atherosclerotic process. We examined the effects in a transgenic rat model of human apoA-I expression on the hyperlipoproteinemia and edema after puromycin aminonucleoside-induced nephrosis in three groups of animals: low line (TgR[hAI]_{low}, human plasma apoA-I = 16.0 mg/dl); high line (TgR[hAI]_{high}, 284 mg/dl); and non-transgenic litter mates (TgR[hAI]_{non}). Nephrosis increased total plasma apoA-I levels 2-fold in TgR[hAI]_{non} rats (75 vs. 162 mg/dl) and 4-fold in the TgR[hAI]_{low} (97 vs. 458 mg/dl) and TgR[hAI]_{high} rats (356 vs. 1,345 mg/dl). In both transgenic lines, this increase was due mainly to elevations of serum human apoA-I. The hepatic steady-state levels of rat apoA-I mRNA increased 5- to 7-fold in all three groups, while human apoA-I mRNA levels increased 21- and 65-fold in the low and high expressing groups, respectively, indicating a different degree of responsiveness of the rat and human genes. While nephrotic TgR[hAI]_{non} and TgR[hAI]_{low} rats showed severe hyperlipoproteinemia and edema, much lower levels of edema and of serum triglycerides, phospholipids, and cholesterol were seen in the TgR[hAI]_{high} group. Urinary excretion of apoA-I, phospholipids, and cholesterol was significantly increased in the TgR[hAI]_{high} group, indicating this as one possible mechanism for the relatively lower serum levels of these lipids. ■ We conclude that the human apoA-I gene is responsive to nephrosis and that human apoA-I-transgenic rats with this syndrome provide an animal model for the study of human high density lipoprotein and apoA-I metabolism.—Burkley, B. F., D. France, H. Wang, X. Ma, B. Brand, C. Abuhani, M. R. Diffenderfer, J. B. Marsh, J. R. Paterniti, Jr., and E. A. Fisher. Overexpression of human apolipoprotein A-I in transgenic rats and the hyperlipoproteinemia associated with experimental nephrosis. *J. Lipid Res.* 1995, 36: 1463–1473.

Supplementary key words high density lipoprotein • kidney disease • puromycin aminonucleoside • hyperlipidemia • proteinuria

Hyperlipoproteinemia is a common feature of the nephrotic syndrome and other glomerular diseases in both humans and experimental animals (1–4). While, in the general population, hyperlipoproteinemia is a strong risk factor for coronary artery disease, in those with renal disease its potential for adverse consequences may be further increased by contributing to the progression of glomerular dysfunction (5).

In previous studies of non-transgenic rats with experimental nephrotic syndrome, a hallmark of the hyperlipoproteinemia has been the overproduction by the liver of apolipoprotein A-I (apoA-I) (4). Thus, in spite of urinary losses of high density lipoprotein (HDL) (6), serum levels of HDL cholesterol typically increase, contributing to the hyperlipidemic state. The overproduction of hepatic apoA-I has been shown to result from increased apoA-I synthesis (7), and in more recent studies this was attributed to increased apoA-I gene expression (8–10).

The availability of transgenic rats expressing human apoA-I (h-apoA-I) (11) allowed us to determine whether the human gene also responds to the nephrotic state. In addition, by studying lines with different quantitative levels of basal h-apoA-I expression (low and high), we were able to explore relationships among the degree of h-apoA-I production, the serum levels of apoA-I and apoB-containing lipoproteins, and the severity of the nephrotic state.

Abbreviations: TgR, transgenic rat; FPLC, fast protein liquid chromatography; TBS, Tris-buffered saline; PAN, puromycin aminonucleoside; h-apoA-I, human apolipoprotein A-I.

¹Reprint requests may be addressed to either author.

The results demonstrate that the h-apoA-I gene responded to the nephrotic syndrome in each transgenic group (low and high basal expressors). Furthermore, when nephrosis was induced in the group with high basal expression, compared to non-transgenic controls and low expressors, there was suppression of edema and less hyperlipoproteinemia, associated with increased urinary excretion of apoA-I, cholesterol, and phospholipids. Thus, in addition to the value of these two groups of transgenic rats to studies of lipid and apolipoprotein metabolism, their differing responses to nephrosis could potentially be used to test the effects of plasma lipid and lipoprotein levels on the progression of glomerular dysfunction in experimental renal disease.

MATERIALS AND METHODS

Induction of experimental nephrosis

Transgenic rats were generated by microinjection of a 13 kbp DNA fragment containing the human apoA-I gene plus 10 kbp of 5' and 1 kbp of 3' flanking sequence. Two established transgenic rat lines, TgR[0hAI]7 and TgR[0hAI]2, express moderate and high levels of h-apoA-I, respectively. Both lines were originally made using OFA rats (Oncins France Strain A derived from the Sprague-Dawley strain) and subsequently rederived to a Sprague-Dawley background (11). TgR[0hAI]7 will be referred to as TgR[hAI]_{low}, TgR[0hAI]2 will be referred to as TgR[hAI]_{high}, and non-transgenic littermates will be referred to as TgR[hAI]_{non}. Male rats, 10 per group, age 7–11 weeks were used. In each group, experimental nephrosis was induced in one-half of the rats by bolus intraperitoneal injections of puromycin aminonucleoside (PAN) at 65 mg/kg body weight (No P-7103; Sigma Chemical Co., St. Louis, MO) in saline, on 2 consecutive days. All other animals were injected with equivalent volumes of saline. Within 8 days, the response to PAN treatment was readily apparent as peritoneal edema, which could be clinically graded (by a blinded observer) over a range of slight to severe. Animals were killed 8 days after the initial injection of PAN or saline. Whole blood for serum isolation and livers were collected at the time of killing. In a separate experiment, urine was collected from four TgR[hAI]_{non} and four TgR[hAI]_{high} rats by placing them in metabolic cages 20 h prior to killing. All animal studies were performed under a protocol approved by the Animal Care Committee of the Medical College of Pennsylvania and the Sandoz Animal Care and Use Committee.

Serum lipid analysis

One part of serum was diluted with four parts of distilled water for the analysis of total serum cholesterol, triglyceride, and phospholipid. In a 96-well microplate (Nunc-Immuno Plate MaxiSorb, InterMed) 25 μ L of diluted serum was assayed for its lipid content by the addition of 200 μ L cholesterol reagent (No. 352-1000, Cholesterol 1000, Sigma), or 200 μ L triglyceride reagent (No. 450032; Triglycerides/GB, Boehringer Mannheim Co., Indianapolis, IN), or 200 μ L phospholipid reagent (No. 996-54001; Phospholipids B, Wako Pure Chemical Industries, Osaka Japan) as specified by the manufacturers. Samples were developed by incubating for 30 min at room temperature and absorbance was determined at 490 nm. Equivalent dilutions of calibrated lipid standards (No. C 0534, Cholesterol Calibrator Set, Sigma) and calibrated controls (No. L 1008, Lipid Control-E and No. L 2008, Lipid Control-N, Sigma) were used as reference standards. Fractionation of serum lipoproteins by Superose-6 gel permeation chromatography was performed with a robotic FPLC system as previously described (12). Briefly, the column matrix was equilibrated with Tris-buffered saline (TBS, 50 mM Tris, pH 7.4, 0.15 M NaCl) containing 0.01% sodium azide at 0.5 mL per min. Serum, 200 μ L, was injected and 40 0.5-mL fractions were collected at a flow rate of 0.5 mL/min. The cholesterol profile was determined on an 80- μ L fraction with 120 μ L of cholesterol reagent (No. 81423, Fast Cholesterol, Sclavo, Wayne, NJ). After incubation at room temperature for 30 min, absorbance was determined at 490 nm.

Urine lipid analysis

Rats were placed in individual metabolic cages and urine was collected overnight. Aliquots were analyzed for cholesterol and phospholipids. Proteins were first precipitated with 10% trichloroacetic acid and the precipitates were extracted twice at room temperature with 1% trichloroacetic acid in ethanol. The precipitates were dissolved in 0.1 N NaOH and protein concentrations were measured by the micro-biuret method (13).

The supernatant solution was treated with 3 volumes of ether to precipitate the acid-alcohol-soluble protein. The protein was dissolved in 0.1 N NaOH and its concentration was determined (13). The solvents were removed from the lipid extract, which was then re-dissolved in chloroform-methanol 2:1. Water-soluble substances were removed by the method of Folch, Lees, and Sloane Stanley (14). Cholesterol and phospholipid in the chloroform phase of the Folch extract were determined by the methods of Zlatkis, Zak, and Boyle (15) and Sokoloff and Rothblat (16), respectively.

Nondenaturing gradient gel electrophoresis of serum lipoproteins

Total lipoproteins from 200 μ L serum, adjusted to d 1.23 g/mL with potassium bromide, were isolated by a 12-h (42,000 rpm) single-spin density ultracentrifugation in a Ti42.2 rotor (Beckman Instruments, Palo Alto, CA). Two parts of lipoprotein fraction (the upper 60 μ L sample from the spin) were mixed with one part of Sudan Black B (7 mg/mL in polyethylene glycol) and incubated at room temperature for 2 h. Lipoproteins from 20 μ L were loaded onto a nondenaturing polyacrylamide gradient gel (PAA 2/16; Pharmacia LKB, Uppsala, Sweden) and resolved by electrophoresis at 125 V for 16 h in 89 mM Tris, pH 8.3, 89 mM boric acid, and 2.6 mM EDTA (No. SA 100033, TBE Seprabuff, Integrated Separation Systems, Natick, MA). After lipid-containing bands were identified, apolipoproteins and molecular weight markers were visualized by staining with Coomassie Brilliant Blue (No. B-8647, Brilliant Blue R, Sigma).

Quantitation of serum apoA-I

Levels of human and rat apoA-I were determined by competition ELISA. For the h-apoA-I assay, microplate wells (Nunc-Immuno Plate MaxiSorb, Baxter Scientific, Edison, NJ) were coated overnight at 4°C with 0.4 μ g per well of purified h-apoA-I (No. A-9284, Sigma), then blocked for 2 h at room temperature in TBS containing 5% bovine serum albumin (BSA). Assay plates were incubated overnight at room temperature with rat serum diluted 1:20 in TBS containing 4% Tween-20 (preheated to 52°C, 1 h) and goat anti-human apoA-I immune serum diluted 1:10,000 in TBS containing 4% Tween-20. Anti-human apoA-I immune serum was generated by immunizing a goat with h-apoA-I isolated from human HDL₃ and purified by electroelution of a single band from an SDS polyacrylamide gel (17). After washing, bound anti-human apoA-I antibodies were tagged with alkaline phosphatase-conjugated rabbit anti-goat IgG (No. A-7650, Sigma) diluted 1:1,000 in TBS containing 2% BSA and detected using 200 μ L of a 1 mg/mL phosphatase substrate (No. 104-0, Sigma) dissolved in 2% diethanolamine. After incubation at room temperature for 30 min, the absorbance was determined at 405 nm. Standard curves were made by serial dilution of human serum containing known amounts of h-apoA-I. There was no detectable cross-reactivity (by either immunoblot or ELISA format) of the anti-human apoA-I immune serum for rat apoA-I. The assay was linear over the range of 1.5–24 μ g apoA-I per well.

The rat apoA-I ELISA was identical to the above ELISA, except 800 ng of rat apoA-I, purified from rat HDL by preparative SDS PAGE (17), was used to coat each well of the microtiter plate. Diluted rat serum

samples were not preheated, and goat anti-rat apoA-I immune serum was diluted 1:7,500. Anti-rat apoA-I immune serum was generated by immunizing a goat with rat apoA-I isolated from rat HDL₃ and purified by electroelution of a single band from an SDS polyacrylamide gel (17). Standard curves were made by dilution of rat serum containing known amounts of rat apoA-I. Minor cross-reactivity of anti-rat apoA-I antiserum for h-apoA-I was removed by affinity chromatography over a human serum affinity column. The assay was linear in the range of 0.9–15 μ g of apoA-I per well.

Non-reducing SDS-PAGE analysis of serum and urine proteins

Rat serum or urine (3 μ L) was mixed into Tris-SDS sample solubilization buffer (No. SA100051, Tris-SDS SepraSOL, Integrated Separation Systems) to yield a 50 μ L final volume. Samples were heat-denatured at 80°C for 15 min, and loaded on an 11% SDS polyacrylamide gel. Proteins, resolved by electrophoresis at 75 V for 6 h, were visualized by staining with Coomassie Brilliant Blue.

Density gradient ultracentrifugation of total serum lipoproteins

Pools of serum (1 mL) from each treatment group were density adjusted to 1.23 g/mL with potassium bromide in 14 \times 95 mm polyallomer centrifuge tubes (No. 331374, Beckman). Four potassium bromide solutions of descending density from 1.15 to 1.01 g/mL were layered over the serum sample and ultracentrifuged in a Beckman SW40Ti rotor at 35,000 rpm for 36 h at 4°C. Lipoproteins were collected by pumping a 1.30 g/mL potassium bromide solution at a rate of 0.4 mL/min through a 20-gauge needle inserted through the tube wall at the bottom of the centrifuge tube. Fractions of 0.2 mL were collected for analysis of total cholesterol, h-apoA-I and rat apoA-I.

Isolation and analysis of hepatic RNA

Total RNA was isolated from rat liver by a modified guanidine salt-based procedure previously described (18). Ten- μ g aliquots of RNA were mixed in loading buffer (50% formamide, 16% formaldehyde, 50 mM MOPS, 2 mM EDTA, pH 7.0), heated to 56°C for 30 min, rapidly chilled on ice, and electrophoresed at 50 V for 3–5 h on a 1% agarose gel containing 17.75% formaldehyde, 50 mM MOPS, 2 mM EDTA, pH 7.0. Resolved RNA was transferred to a nylon membrane (ZetaProbe, Bio-Rad, Melville, NY) by passive capillary transfer in 50 mM NaOH and UV crosslinked. Oligonucleotide probes complementary to the rat and human apoA-I mRNAs were labeled by the T4 polynucleotide kinase technique (19) with [γ ³²P]ATP (3000 Ci/mmol, New England Nu-

clear, Boston, MA). All blots were prehybridized for 4–5 h at 65°C in 5 × SSC, 20 mM sodium phosphate, pH 7.0, 10 × Denhardt's solution, 7% SDS, with 100 µg/mL denatured salmon sperm DNA. Heat-denatured probes were hybridized to the immobilized RNA at 65°C in hybridization buffer (the same as prehybridization buffer, but with the addition of 10% dextran sulfate). The blots were washed twice with 0.5 × SSC, 0.1% SDS at room temperature, then once with 0.1 × SSC, 0.1% SDS at 65°C. Blots were then exposed to a phosphor screen overnight and scanned on a Molecular Dynamics Phosphorimager. The intensity of the hybridization signal was normalized to elongation factor 1 α , as described by Lu and Werner (20), and expressed as relative to this control.

Values are given as the mean \pm standard error of the mean. Statistical differences between treatment groups were sought by using Student's *t* test.

RESULTS

Rat and human apoA-I protein and mRNA levels

As previously reported (21, 22), total serum apoA-I increased after the induction of nephrosis (Table 1). However, a more pronounced total apoA-I elevation occurred in TgR[hAI]_{low} and especially in TgR[hAI]_{high} nephrotic rats, where apoA-I replaced albumin as the major serum protein (see Fig. 4A). The increase in total apoA-I in the TgR[hAI]_{low} and TgR[hAI]_{high} nephrotic rats was primarily due to increased h-apoA-I levels. Rat

apoA-I actually decreased in the nephrotic TgR[hAI]_{high} group.

We have shown previously that the genetic construct used to produce TgR[hAI]_{low} and TgR[hAI]_{high} rats drove the expression of h-apoA-I in the liver but not in the intestine (11). Hepatic rat and human apoA-I mRNA levels were measured by Northern blot hybridization in control and nephrotic rats (Fig. 1 and Table 2). Similar to previous reports (8–10), the induction of experimental nephrosis significantly increased the steady-state levels of rat apoA-I mRNA (5- to 7-fold) over the controls. By contrast, h-apoA-I mRNA levels were elevated 21-fold in TgR[hAI]_{low} rats and 65-fold in TgR[hAI]_{high} rats. These data demonstrate that rat and h-apoA-I mRNA and protein were differentially elevated by the induction of experimental nephrosis.

Effects of human apoA-I on PAN-induced hyperlipoproteinemia

In control TgR[hAI]_{high} rats, expression of h-apoA-I was associated with raised circulating levels of cholesterol (51.2%) and phospholipid (66.5%) compared with TgR[hAI]_{non} rats, while triglycerides were unchanged. The increased serum levels of cholesterol and phospholipid in TgR[hAI]_{high} rats reflected expansion of the HDL pool, evident in the FPLC lipoprotein cholesterol profile of Fig. 2A, and were consistent with our previous report (11). The minor contribution of h-apoA-I in the control TgR[hAI]_{low} rats was not enough to alter total serum lipid and lipoprotein profiles.

Consistent with the model of experimental nephrosis (4), marked elevations of total cholesterol (+460%), phospholipid (+212%), and triglyceride (+627%) occurred in TgR[hAI]_{non} rats after PAN induction. The degree of lipid elevation in nephrotic TgR[hAI]_{non} rats and nephrotic TgR[hAI]_{low} rats was virtually identical (Table 3). By contrast, the induction of experimental nephrosis in TgR[hAI]_{high} animals produced only a modest elevation (+52%) of total serum cholesterol and actually decreased phospholipid levels (Table 3). Total serum triglyceride increased 219% (control: 70.1 mg/dL vs. nephrotic: 223.7 mg/dL). However, this elevation was less than one-half of the response of nephrotic TgR[hAI]_{non} or TgR[hAI]_{low} rats, and was not statistically significant (*P* = 0.092). Thus, overexpression of h-apoA-I in the TgR[hAI]_{high} rats suppressed the hyperlipoproteinemia associated with experimental nephrosis.

To obtain lipoprotein profiles, serum samples were fractionated by FPLC gel permeation chromatography and lipoprotein peaks were determined by elution volume and cholesterol content. In control TgR[hAI]_{non} rats, HDL was the predominant lipoprotein species (Fig. 2A). Induction of experimental nephrosis resulted in

TABLE 1. Rat and human apoA-I serum levels 8 days after PAN (nephrotic) or saline (control) injection

Group	Serum ApoA-I Levels		
	Rat ApoA-I	Human ApoA-I	Total ApoA-I
	mg/dL		
TgR[hAI] _{non}			
Control	75.2 \pm 10.0		75.2 \pm 10.0
Nephrotic	162.4 \pm 26.6		162.4 \pm 26.6
N/C	2.16 ^a		2.16 ^a
TgR[hAI] _{low}			
Control	81.2 \pm 10.4	16.0 \pm 4.7	97.2 \pm 8.7
Nephrotic	127.4 \pm 9.1	330.8 \pm 51.7	458.2 \pm 44.0
N/C	1.57 ^a	20.68 ^b	4.71 ^b
TgR[hAI] _{high}			
Control	71.8 \pm 17.7	284.2 \pm 113.4	356.0 \pm 96.1
Nephrotic	38.3 \pm 5.9	1307.5 \pm 186.0	1345.8 \pm 191.3
N/C	0.53 ^c	4.60 ^b	3.78 ^b

Human and rat apoA-I were measured by species-specific competition ELISA. Values are given as mean \pm SEM, *n* = 5; total apoA-I is the sum of rat and human values. The change from control in each group is expressed as the ratio of N/C (nephrotic/control).

^a*P* < 0.05; ^b*P* < 0.005; ^cno significant difference, where the two groups are statistically different as determined by Student's *t*-test.

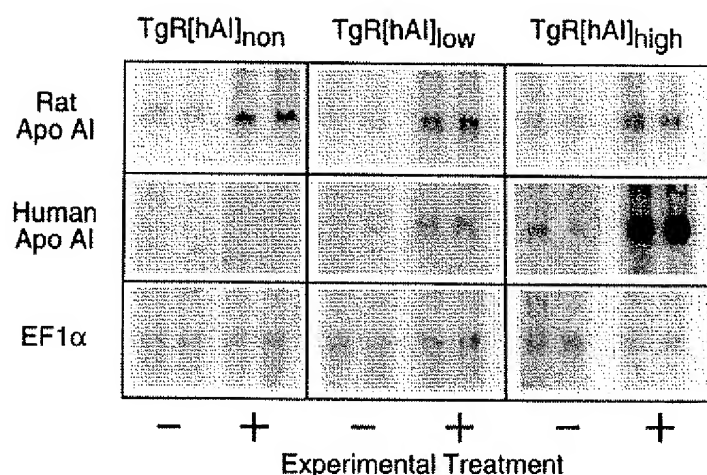


Fig. 1. Northern blot analysis of hepatic rat apoA-I, human apoA-I, and rat EF1 α . Total RNA was isolated from livers of TgR[hAI]_{non}, TgR[hAI]_{low}, and TgR[hAI]_{high} rats killed 8 days after PAN or saline injection. Ten micrograms per lane of total RNA was resolved using a formaldehyde-denaturing gel, transferred to nitrocellulose, and hybridized with rat-specific apoA-I, human-specific apoA-I, or EF1 α radio-labeled probes. Each experimental group, PAN (+) or saline (-) injected rats, is represented by two individuals within each group.

hyperlipoproteinemia evident as increases of all lipoprotein classes. Lipoprotein profiles of TgR[hAI]_{low} control and nephrotic rats (data not shown) were virtually identical to the corresponding profiles of TgR[hAI]_{non} rats shown in Fig. 2A. Overexpression of h-apoA-I in TgR[hAI]_{high} control rats expanded the HDL cholesterol pool (compare Figs. 2A and 2B). While some increase in non-HDL cholesterol fractions occurred in TgR[hAI]_{high} rats with experimental nephrosis, hyperbeta-lipoproteinemia was decreased (compare Figs. 2A and 2B). Surprisingly, in the face of large differences of total serum apoA-I, HDL cholesterol levels in TgR[hAI]_{high} rats were unchanged in controls (142.4 ± 33.4 mg/dL)

versus in nephrotics (140.5 ± 21.2 mg/dL). However, HDL particles isolated from TgR[hAI]_{high} nephrotic animals tended to elute ahead of control HDL on FPLC, indicating an increased particle size.

The HDL particle size distribution was further examined by non-denaturing gradient gel electrophoresis (Fig. 3). In control TgR[hAI]_{non} and TgR[hAI]_{low} rats, a single HDL₂ species was present (23). Control TgR[hAI]_{high} rat HDL was polydisperse with distinct HDL₁-like, small HDL₂, and very small HDL₃ species. In TgR[hAI]_{non} and TgR[hAI]_{low} rats with experimental nephrosis, two distinct HDL species, comparable to human HDL₂ and HDL₃, were observed. Nephrotic TgR[hAI]_{high} rat serum contained only large particles that displayed size heterogeneity among individual rats. Smaller HDL particle classes were absent in these animals.

Effect of overexpression of human apoA-I on albuminemia, edema, and urine composition in PAN-treated rats

Eight days after the initial injection of PAN, rats were killed and serum proteins were resolved on a non-reducing SDS polyacrylamide gel (Fig. 4A). Hypoalbuminemia was evident in all three PAN-treated groups. Additionally, upon killing, all rats receiving PAN displayed peritoneal edema while their saline-treated counterparts appeared normal. The edema in all TgR[hAI]_{high} nephrotic rats, however, was clinically less severe than that observed in nephrotic TgR[hAI]_{low} and TgR[hAI]_{non} animals. Urine from control (saline-treated) and nephrotic TgR[hAI]_{non} and TgR[hAI]_{high} rats was collected for a 20-h period prior to killing. Urine protein excretion was low from two saline-treated TgR[hAI]_{non} rats (0.54 and 0.55 mg/h) as well as from two saline-treated TgR[hAI]_{high} rats (0.77 and 0.59 mg/h). As expected, significant proteinuria was detected in two PAN-treated TgR[hAI]_{non} rats, 5.18 and

TABLE 2. Levels of hepatic human and rat apoA-I mRNA 8 days after PAN (nephrotic) or saline (control) injection as determined by Northern blot analysis

Group	Hepatic ApoA-I mRNA	
	Rat ApoA-I	Human ApoA-I
TgR[hAI] _{non}		
Control	0.41 \pm 0.04 (3)	
Nephrotic	2.49 (2.28, 2.70)	
N/C	6.1	
TgR[hAI] _{low}		
Control	0.45 \pm 0.15 (4)	0.15 \pm 0.06 (4)
Nephrotic	3.24 \pm 0.25 (4)	3.16 \pm 0.27 (4)
N/C	7.2	21.1
TgR[hAI] _{high}		
Control	0.35 \pm 0.06 (4)	1.19 \pm 0.80 (4)
Nephrotic	1.79 (1.91, 1.67)	77.03 (80.4, 73.7)
N/C	5.1	64.7

Rat and human apoA-I mRNA levels in livers were determined using species-specific oligonucleotide probes and are expressed as phosphorimager units normalized to constitutively expressed Elongation Factor 1 alpha (EF1 α). Each value is the mean \pm SEM, with the number (n) in parentheses, except where the n was less than 3, when the average of two determinations (values in parentheses) is given. The change from the control in each group is expressed as the ratio of nephrotic/control (N/C).

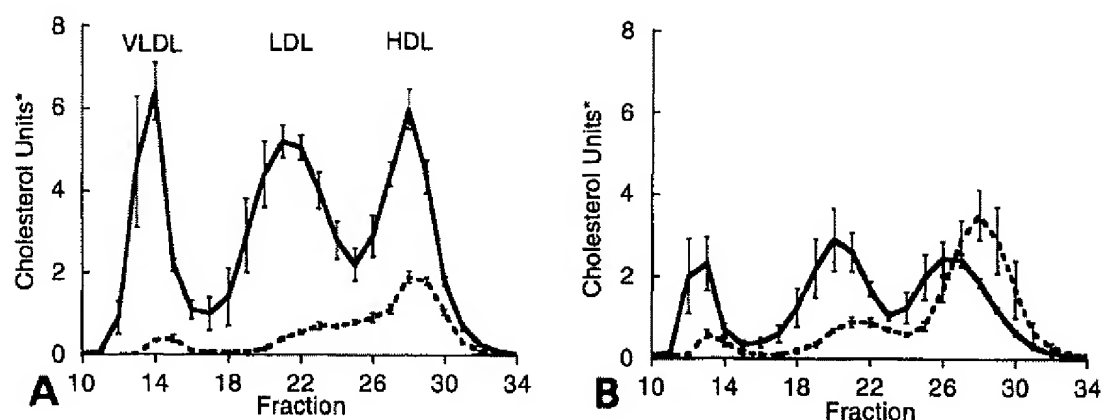


Fig. 2. Analysis of lipoprotein profiles from TgR[hAI]_{low} (A) and TgR[hAI]_{high} (B) rat sera by gel filtration chromatography. Individual rat serum samples were fractionated by FPLC over a Superose 6 sizing column into 40 fractions. Total cholesterol from each fraction was assessed enzymatically, the absorbance at 490 nm* was assigned whole-number values using a linear relation and the profiles were plotted. Dashed lines (—) are saline-injected control rats and solid lines (—) are PAN-injected nephrotic rats. Each profile is the mean of five individual profiles, with error bars representing the standard error of the mean. The elution positions of human VLDL, LDL and HDL are indicated at the top of each profile.

11.42 mg/h. However, the proteinuria was considerably greater in two PAN-treated TgR[hAI]_{high} rats, 20.85 and 27.36 mg/h. Analysis of the urine proteins by non-reducing SDS PAGE (Fig. 4B) shows that much of the protein eliminated in the urine of PAN-treated TgR[hAI]_{non} rats is albumin, whereas in PAN-treated TgR[hAI]_{high} rats, the albumin band has reduced intensity and the apoA-I band becomes more prominent. In a separate set of urine samples, lipid excretion was measured. As shown in Table 4, the urine concentrations of both phospholipid and cholesterol were signifi-

cantly increased in the PAN-treated TgR[hAI]_{high} rats relative to those in the PAN-treated TgR[hAI]_{non} rats.

Effect of human apoA-I overexpression on cholesterol and apolipoprotein density class distribution

To better define the circulating form of apoA-I, serum lipoproteins were resolved by continuous gradient density centrifugation. Rat and human apoA-I distributions were determined across gradient fractions by ELISA. In saline-treated TgR[hAI]_{non} rats, rat apoA-I was found exclusively in the HDL density range (1.063–1.21 g/mL). This pattern persisted after the induction of nephrosis (data not shown). In saline-treated TgR[hAI]_{low} rats, both the rat and human apoA-I were found in the HDL density range (Fig. 5A). After the induction of nephrosis in TgR[hAI]_{low} rats, the human apoA-I partitioned mainly into HDL (Fig. 5B), but approximately one-half of the rat apoA-I was now associated with density > 1.21 g/mL fraction. This distribution of human and rat apoA-I was also observed in TgR[hAI]_{high} control rats (Fig. 5C). One possibility suggested by these results is that with sufficiently high levels of expression of h-apoA-I (nephrotic TgR[hAI]_{low} or non-nephrotic TgR[hAI]_{high} rats), rat and human apoA-I compete for the available lipid pool, and that h-apoA-I may be bound tighter to HDL particles than rat apoA-I, allowing for dissociation from HDL particles upon centrifugation. In nephrotic TgR[hAI]_{high} rats, with the greatest expression of h-apoA-I (circulating levels > 1300 mg/dL, Table 1), the h-apoA-I was distributed across three peaks (Fig. 5D). The first peak corresponded to a

TABLE 3. Effect of human apoA-I overexpression on levels of triglyceride, phospholipid, and cholesterol in serum from rats 8 days after PAN (nephrotic) or saline (control) injection

Group	Serum Lipid Levels		
	Triglyceride	Phospholipid	Cholesterol
	mg/dL		
TgR[hAI] _{non}			
Control	78.3 ± 11.5	201.4 ± 6.7	116.9 ± 5.0
Nephrotic	568.9 ± 49.1	627.8 ± 49.3	654.9 ± 52.3
N/C	7.27 ^a	3.12 ^a	5.60 ^a
TgR[hAI] _{low}			
Control	70.0 ± 11.4	186.3 ± 9.0	110.6 ± 7.2
Nephrotic	505.7 ± 54.8	536.2 ± 45.7	569.3 ± 71.0
N/C	7.22 ^a	2.88 ^a	5.15 ^a
TgR[hAI] _{high}			
Control	70.1 ± 10.7	304.4 ± 43.8	194.5 ± 35.6
Nephrotic	223.7 ± 68.9	202.4 ± 56.1	296.1 ± 41.4
N/C	3.19 ^b	0.67 ^b	1.52 ^b

Values given as mean ± SEM, n = 5. The change from control in each group is expressed as the ratio of nephrotic/control (N/C).

^aP < 0.001; ^bno significant difference, when the two groups are statistically different by Student's *t*-test.

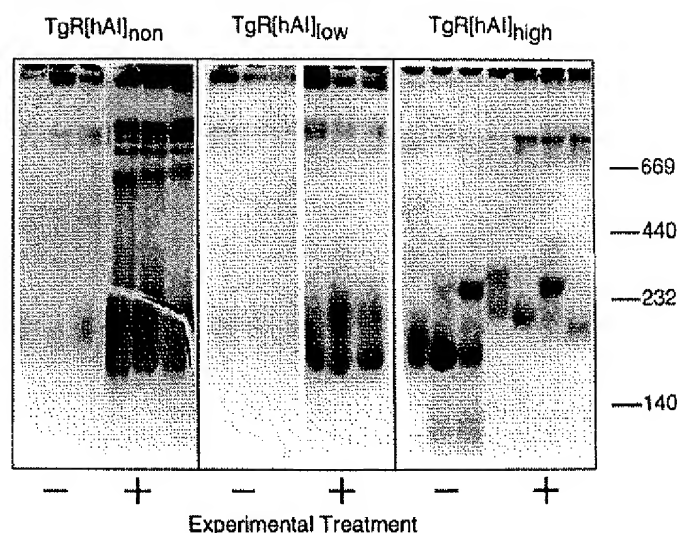


Fig. 3. Non-denaturing gradient gel analysis of total lipoproteins isolated from TgR[hAI]_{non}, TgR[hAI]_{low}, and TgR[hAI]_{high} rat serum by single spin 1.23 g/mL density centrifugation. Lipoprotein fractions, preincubated 2 h with Sudan black 7B to stain neutral lipids, were resolved on PPA 2/16 nondenaturing gradient gels. The prestained lipoprotein profiles were photographed and the gels were then stained and destained in Coomassie Brilliant Blue to develop the molecular weight standards, shown at the right as $M_r \times 10^3$. Each experimental treatment group, PAN (+) and saline (-) injected, is represented by three individuals, except the TgR[hAI] Pan-treated group that contains four.

buoyant HDL population that co-eluted with a major cholesterol peak, the second one, a denser HDL population co-eluting with a minor cholesterol peak, and the third, a lipid-free or poor population with density > 1.21 g/mL. Rat apoA-I was now found mainly in the density range > 1.21 g/mL. Thus, the induction of experimental nephrosis in TgR[hAI]_{high} rats resulted in significant proportions of the serum pools of both rat and human apoA-I appearing in the non-lipoprotein density fraction.

DISCUSSION

Effects of overexpression of human apoA-I on edema in experimental nephrosis

The mechanisms underlying fluid volume expansion in the nephrotic syndrome have been studied extensively (24). Hypoalbuminemia decreases plasma oncotic pressure, antagonizing forces in the venular capillary that counteract hydrostatic pressure. Fluid balance is further deranged by changes in capillary permeability

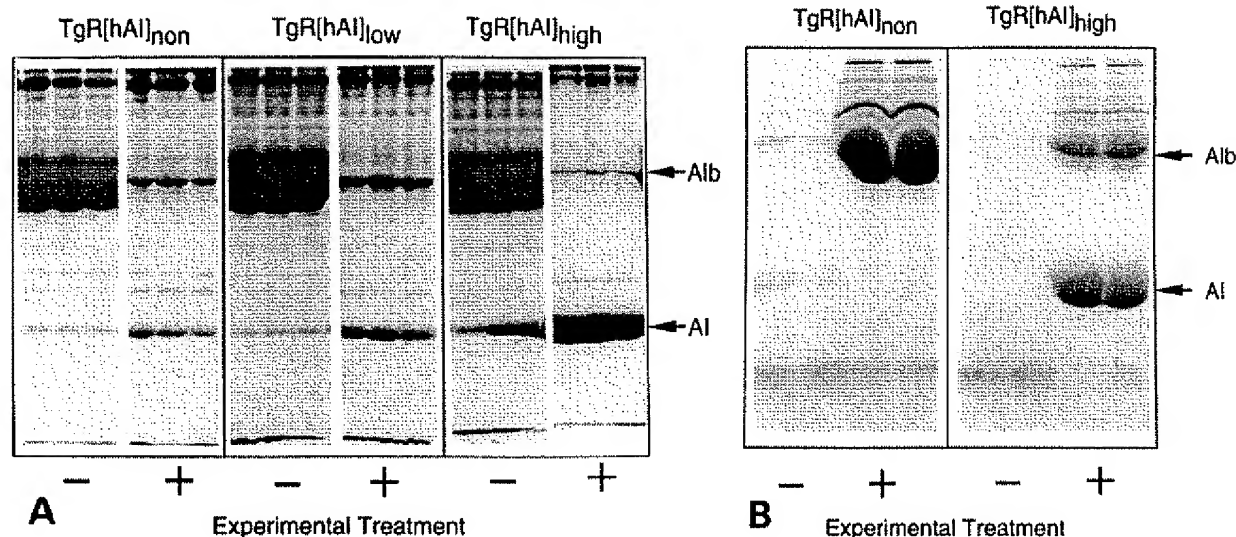


Fig. 4. Analysis of total serum and urine proteins by non-reducing SDS-PAGE. Total proteins from 3 μ L of serum (A) or 5 μ L of urine (B) per rat were resolved on an 11% non-reducing SDS polyacrylamide gel. The resolved proteins were visualized with Coomassie Brilliant Blue R-250. The locations of albumin and apoA-I bands are indicated to the right. Each experimental group (PAN (+) or saline (-) injected) is represented by three serum samples (panel A) and two urine samples (panel B) from individuals within each group.

TABLE 4. Urine lipid concentrations in nephrotic rats

Group	Urine Lipid Levels	
	Phospholipid	Cholesterol
	$\mu\text{g/mL}$	
TgR[hAI] _{low}		
Nephrotic (n = 3)	235.0 \pm 18.7	162.0 \pm 14.3
TgR[hAI] _{high}		
Nephrotic (n = 6)	870.0 \pm 152.0	348.0 \pm 43.2

Experimental nephrotic syndrome was induced in TgR[hAI]_{low} and TgR[hAI]_{high} rats and urine samples were collected in metabolic cages. Total proteins were precipitated and quantitated. Lipids were extracted by the Folch procedure and cholesterol and phospholipid contents of the extracts were determined. Values are given as mean \pm SEM. The urine protein concentrations averaged 43 ± 1.09 and 33 ± 2.87 mg/mL in the TgR[hAI]_{low} and TgR[hAI]_{high} groups, respectively. $P < 0.03$ for the group differences in cholesterol and phospholipid.

and an increased natriuretic peptide activity (25). Intravenous administration of albumin or other plasma ex-

pander macromolecules will decrease edema, at least temporarily (26). Earlier work in humans with nephrotic syndrome has shown that plasma lipid levels will also decline when plasma expanders are given (27).

In nephrotic animals, overexpression of human apoA-I did not prevent hypoalbuminemia (Fig. 1) or albuminuria (Fig. 4B). Extreme overproduction of h-apoA-I in the PAN-treated TgR[hAI]_{high} animals was associated with decreased edema in the nephrotic state. This can be most simply explained by the support of plasma oncotic pressure by the high serum levels of apoA-I. In other words, in spite of the urinary losses of apoA-I (Fig. 4B and ref. 28), hepatic apoA-I production was so increased that the serum level reached 1346 mg/dL. Given the relative molecular weights of albumin (67 kD) and apoA-I (28 kD), this level of apoA-I would exert an oncotic pressure corresponding to 3.2 g/dL of albumin, which is within the normal plasma range. Though this calculation assumes that all apoA-I was in the free or lipid-poor state ($d > 1.21$) and this was not strictly the

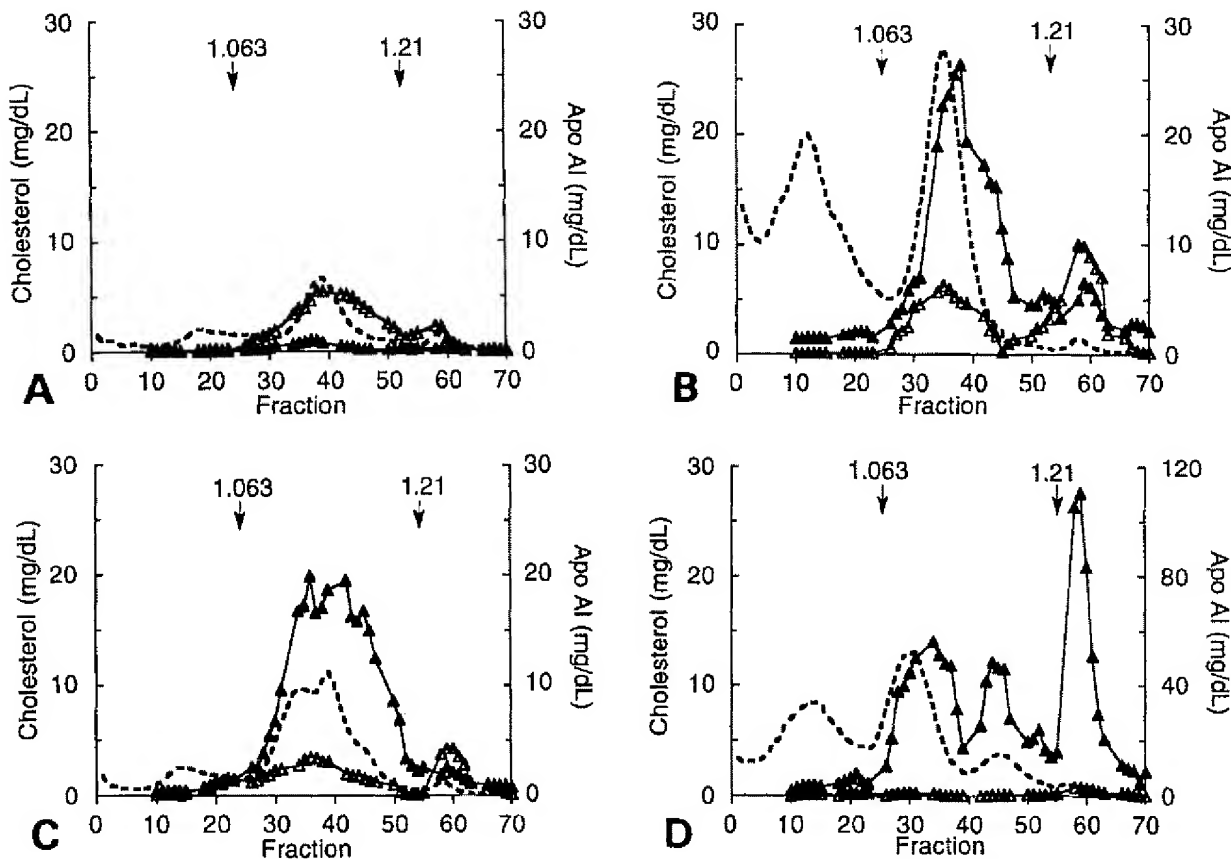


Fig. 5. Distribution of apoA-I and cholesterol by density gradient ultracentrifugation. Pooled sera from A) TgR[hAI]_{low} saline-injected, B) TgR[hAI]_{low} PAN-injected, C) TgR[hAI]_{high} saline-injected, and D) TgR[hAI]_{high} PAN-injected groups were subjected to density gradient ultracentrifugation. Profiles were fractionated for the analysis of total cholesterol (—), rat apoA-I (---), and human apoA-I (---). The densities of the fractions were determined and reference densities 1.063 g/mL and 1.21 g/mL are shown above each profile.

case, nonetheless, a large fraction of apoA-I in nephrotic TgR[hAI]_{high} rats was indeed found in the $d > 1.21$ fraction of serum (Fig. 5D). In contrast, while nephrotic TgR[hAI]_{low} rats expressed over 450 mg/dL of apoA-I, almost all of it was associated with HDL particles (Fig. 5B). Thus, because of both the lower concentration of serum apoA-I and its presence predominantly in a form (HDL) that contributes little to oncotic pressure, it is not surprising that in contrast to nephrotic TgR[hAI]_{high} rats, these animals showed the same degree of edema as the non-transgenic nephrotic controls.

Effects of experimental nephrosis on apoA-I gene expression

Although the detailed molecular mechanisms underlying the hepatic response to the nephrotic syndrome are unknown, there is an increased steady-state level of apoA-I mRNA upon the induction of nephrosis in rats (8–10). As the apoA-I mRNA level is a critical determinant of apoA-I production rate (29, 30), an increased level of apoA-I mRNA most likely explains the elevated synthesis and secretion of hepatic apoA-I observed in nephrotic rats (7).

In the present study, non-nephrotic animals in all three lines had essentially identical levels of rat hepatic apoA-I mRNA (Table 2). In agreement with the literature (8–10), after the induction of nephrosis, these levels rose significantly (5- to 7-fold) in all the groups. There were also effects of nephrosis on the expression of the h-apoA-I mRNA. PAN treatment resulted in elevations of h-apoA-I mRNA of 21-fold in TgR[hAI]_{low} and 65-fold in TgR[hAI]_{high} animals. Thus, both transgenic lines showed a striking differential response of rat and human apoA-I mRNA levels to experimental nephrosis, with increased sensitivity of the human mRNA.

Prior studies in the PAN nephrosis model (8), the Heymann nephritis model, and the Nagase analbuminemic rat (10) indicated that elevation of rat hepatic apoA-I mRNA was associated with an increased transcriptional activity of the apoA-I gene. This is most likely also to be the basis for the increase in the h-apoA-I mRNA in the transgenic livers, as preliminary experiments (L. Sambucetti and E. A. Fisher, unpublished observations) indicate that the stability of the human apoA-I message was not changed in nephrosis. Why the human gene may be more sensitive than the rat gene to transcriptional activation is currently under study. Hypotheses include activation of additional transcription units in a high-copy cluster of tandemly repeated human apoA-I genes, increased efficacy of rodent factors to *trans*-activate the heterologous human *cis*-elements, and regulatory information in the 5'-flanking sequence of the human gene not present in the rat gene. Nonetheless, despite the need for additional studies to elucidate

molecular mechanisms, the present results clearly demonstrate for the first time that the human apoA-I gene responds in the experimental nephrotic syndrome.

Effects of apoA-I overexpression on apoA-I and lipoprotein metabolism in nephrotic rats

Rubin et al. (31) have reported that in transgenic mice expressing human apoA-I there is a decrease in the serum level of mouse apoA-I. They hypothesized that HDL containing both species of apoA-I are unstable, and this instability leads to the selective loss of mouse apoA-I. In this study, TgR[hAI]_{high} control rats displayed an inverse relationship between circulating levels of rat and human apoA-I ($r^2 = -0.97$, $P < 0.005$, $n = 5$). This line of rats normally displays a significant decrease of rat apoA-I levels when h-apoA-I becomes greater than 200 mg/dl (unpublished data). TgR[hAI]_{low} rats rendered nephrotic had circulating levels of h-apoA-I in excess of 300 mg/dl, yet rat apoA-I levels did not decrease, and actually increased significantly (Table 1). However, TgR[hAI]_{high} rats rendered nephrotic had massive increases in h-apoA-I serum levels and a corresponding decrease (47%) in the level of serum rat apoA-I (Table 1). In the experimental nephrosis model, higher levels of h-apoA-I ($> 1,300$ mg/dl) are needed to observe a decrease in circulating levels of rat apoA-I, possibly reflecting a greater stability of HDL containing rat and human apoA-I as compared to HDL containing the mouse and human proteins. Other potential explanations include differences in the metabolic parameters that impact the forces responsible for displacement of rat apoA-I from HDL, such as the amount of phospholipid associated with apoA-I, the fractional catabolic rate of rat and h-apoA-I, the structure of the nascent apoA-I particle produced by the liver, and alterations in plasma lipase activity associated with nephrosis. Such changes may result in displacement from HDL of rat apoA-I by the large pool of h-apoA-I, with subsequent loss in the urine, or the formation of HDL species, containing rat apoA-I, small enough to be lost in the urine, resulting in the excretion of cholesterol and phospholipids in addition to the apoA-I. Both of these explanations are supported by the gel analysis of urine (Fig. 4), the urine composition analysis (Table 3), and the analyses of serum by non-denaturing gradient gels (Fig. 3) and FPLC (Fig. 5). Associated with the nephrotic state in TgR[hAI]_{high} animals were large urinary losses of apoA-I, cholesterol, and phospholipids and the disappearance from the serum of a small HDL₃-like lipoprotein species. This disappearance could be explained by increased loss of this small particle into the urine. Finally, the FPLC profile demonstrated that a large fraction of the rat apoA-I had a buoyant density > 1.21 , not

associated with HDL and therefore in a form that might be readily lost in the urine.

Nephrotic TgR[hAI]_{non} and TgR[hAI]_{low} rats showed the expected increases in all lipoprotein classes, including triglyceride-rich fractions. However, the results in the TgR[hAI]_{high} rats were dramatically different; although overexpression of h-apoA-I in non-nephrotic TgR[hAI]_{high} rats produced an increase in HDL cholesterol and serum phospholipid (compared to non-nephrotic animals of the other two groups), no further increase in HDL cholesterol was observed after PAN treatment (Table 2). In addition, triglyceride and non-HDL cholesterol levels showed only modest increases with nephrosis, and the associated lipoprotein peaks were blunted (Table 3 and Fig. 3).

Reasoning similar to that just discussed above (i.e., increased urinary losses of HDL or its components) may also explain these results. Alternatively, it is also possible that they reflect a smaller than expected increase in the hepatic production of lipoproteins in nephrotic TgR[hAI]_{high} rats. One potential explanation for this is found in the work of Appel et al. (32), who have shown a significant inverse relationship between plasma cholesterol and oncotic pressure in patients with nephrotic syndrome. This relationship probably reflects a regulatory role of oncotic pressure on hepatic lipoprotein production (10). As the overproduction of apoA-I reduced edema in TgR[hAI]_{high} nephrotic rats, it is reasonable to assume that this was due to the support of oncotic pressure in these animals, perhaps reducing the hepatic stimulation of lipoprotein production by this factor. Another contributing factor is implied by studies by Verkade et al. (33) demonstrating that when newly synthesized phospholipid becomes limiting, there is decreased hepatic secretion of apoB-containing triglyceride-rich lipoproteins. Thus, if the massive overproduction of apoA-I in the nephrotic TgR[hAI]_{high} resulted in a metabolic diversion of phospholipid due to HDL formation, the assembly and secretion of non-HDL lipoproteins may suffer as a consequence. Finally, the overutilization of the protein synthetic machinery, such as ribosomes and translocation channels, by the highest levels of apoA-I production may directly interfere with the translation and processing of other proteins, such as apoB. Though in this section we have offered a number of plausible explanations, many of the issues raised by the urine and serum data, particularly in the nephrotic TgR[hAI]_{high} rats, such as the attribution of results to changes in clearance versus production, are currently being investigated.

Concluding remarks

The induction of the nephrotic syndrome in transgenic rats has demonstrated that the expression of the

human apoA-I gene can be significantly stimulated. Also, a number of effects of this stimulated expression on the metabolism of both HDL and non-HDL lipoproteins were observed. Further investigation of the mechanisms responsible for the effects of nephrosis in transgenic rats expressing h-apoA-I are likely to lead to new insights concerning the regulation of rodent and human apoA-I gene expression as well as the formation and catabolism of lipoproteins. In addition, these animals also represent a potentially useful model for the study of progressive renal disease and its amelioration. For example, we have presented preliminary evidence that apoA-I overexpression in rats decreased smooth muscle cell accumulation in the aorta after balloon injury (34) and Rubin et al. (31) have demonstrated that the overexpression of h-apoA-I in transgenic mice suppressed the formation of aortic foam cells in animals fed an atherogenic diet. Given that a major feature of many models of the atherosclerotic lesion (for example, see ref. 35) is proliferation of smooth muscle cells and accumulation of macrophages, similar to the effects in the aorta, perhaps overexpression of apoA-I in the nephrotic syndrome could also inhibit those changes in glomerular lesions (36) that are hallmarks of the progressive deterioration in renal function. ■

The authors wish to thank Dr. David Weinstein for his helpful comments. This work was supported by grants (to JBM and EAF) from the Howard Heinz Endowment and the National Institutes of Health (HL-22633).

Manuscript received 14 September 1994 and in revised form 30 March 1995.

REFERENCES

1. Keane, W. F., B. L. Kasiske, and M. P. O'Donnell. 1988. Hyperlipoproteinemia and the progression of renal disease. *Am. J. Clin. Nutr.* **47**: 157-160.
2. Wheeler, D. C., V. Zachariah, and J. F. Moorhead. 1989. Hyperlipoproteinemia in nephrotic syndrome. *Am. J. Nephrol.* **9**(suppl 1): 78-84.
3. Kasiske, B. T., M. P. O'Donnell, P. G. Schmitz, Y. Kim, and W. F. Keane. 1990. Renal injury of diet-induced hypercholesterolemia in rats. *Kidney Int.* **37**: 880-891.
4. Marsh, J. B. 1984. Lipoprotein metabolism in experimental nephrosis. *J. Lipid Res.* **25**: 1619-1623.
5. Diamond, J. R., and M. J. Karnofsky. 1992. A putative role of hypercholesterolemia in progressive renal injury. *Annu. Rev. Med.* **43**: 83-92.
6. de Mendoza, S. G., M. L. Kashyap, C. Y. Chen, and R. F. Lutmer. 1976. High density lipoproteinuria in nephrotic syndrome. *Metabolism.* **25**: 1143-1149.
7. Marsh, J. B., and C. E. Sparks. 1979. Hepatic secretion of lipoproteins in the rat and effect of experimental nephrosis. *J. Clin. Invest.* **64**: 1229-1237.
8. Marshall, J. F., J. J. Apostolopoulos, C. M. Brack, and G. J. Howlett. 1990. Regulation of apolipoprotein gene expression and plasma high-density lipoprotein composi-

- tion in experimental nephrosis. *Biochim. Biophys. Acta.* **1042**: 271-279.
9. Tarugi, P., S. Calandra, and L. Chan. 1986. Changes in apolipoprotein A-I mRNA levels in the liver of rats with experimental nephrotic syndrome. *Biochim. Biophys. Acta.* **868**: 51-61.
10. Sun, X., H. Jones, Jr., J. A. Joles, A. Van Tol, and G. A. Kaysen. 1992. Apolipoprotein gene expression in albuminemic rats and in rats with Heymann nephritis. *Am. J. Physiol.* **262**: F755-F761.
11. Swanson, M. E., T. E. Hughes, I. St. Denny, D. S. France, J. R. Paterniti, C. Tapparelli, P. Gfeller, and K. Burki. 1992. High level expression of human apolipoprotein A-I in transgenic rats raises total serum high density lipoprotein cholesterol and lowers rat apolipoprotein A-I. *Transgenic Res.* **1**: 142-147.
12. France, D. S., R. B. Quimby, J. Babiak, D. C. Lapen, R. J. Paterniti, and D. B. Weinstein. 1990. Clinical chemistry applications of microplate robotic systems in a lipoprotein laboratory. *Lab. Robotics & Automation.* **2**: 155-173.
13. Itzhaki, R. F., and D. M. Gill. 1964. A micro-biuret method for estimating proteins. *Anal. Biochem.* **9**: 401.
14. Folch, J. M., M. Lees, and G. H. Sloane Stanley. 1957. A simple method for the isolation and purification of total lipids from animal tissues. *J. Biol. Chem.* **226**: 497-509.
15. Zlatkis, A., B. Zak, and J. A. Boyle. 1953. A new method for the direct determination of serum cholesterol. *J. Lab. Clin. Med.* **41**: 486-492.
16. Sokoloff, L., and G. H. Rothblat. 1974. Sterol to phospholipid molar ratio of L-cells with qualitative and quantitative variations of cellular sterols. *Proc. Soc. Exp. Biol. Med.* **146**: 1166-1172.
17. Brewer, H. B., R. Ronan, M. Meng, and C. Bishop. 1986. Isolation and characterization of apolipoprotein A-I, A-II, and A-IV. *Methods Enzymol.* **128**: 223-246.
18. Zolfaghari, R., X. Chen, and E. A. Fisher. 1993. Simple method for extracting RNA from cultured cells and tissue with guanidine salts. *Clin. Chem.* **39**: 1408-1411.
19. Maniatis, T., E. F. Fritsch, and J. Sambrook. 1982. *Molecular Cloning: a Laboratory Manual.* Cold Spring Harbor Laboratory, Cold Spring Harbor, NY. 122.
20. Lu, X., and D. Werner. 1989. The complete cDNA sequence of mouse elongation factor 1 alpha mRNA. *Nucleic Acids Res.* **17**: 442.
21. Calandra, S., E. Gherardi, M. Fainaru, A. Guaitani, and I. Bartosck. 1981. Secretion of lipoproteins, apolipoprotein A-I and apolipoprotein E by isolated and perfused liver of rat with experimental nephrotic syndrome. *Biochim. Biophys. Acta.* **665**: 331-338.
22. Marsh, J. B., and C. E. Sparks. 1979. Lipoproteins in experimental nephrosis: plasma levels and composition. *Metabolism.* **28**: 455-465.
23. Nichols, A. V., R. M. Krauss, and T. A. Musliner. 1986. Nondenaturing polyacrylamide gradient gel electrophoresis. *Methods Enzymol.* **128**: 417-431.
24. Skorecki, K. L., S. P. Nadler, K. F. Badr, and B. M. Brenner. 1991. Renal and systemic manifestations of glomerular disease. In *The Kidney*. Vol. 1. 4th ed. B. M. Brenner and F. C. Rector, Jr. editors. W. B. Saunders/Philadelphia, Pennsylvania. 891-928.
25. Pericl, N., and G. Remuzzi. 1993. Edema of the nephrotic syndrome: the role of the atrial peptide system. *Am. J. Kidney Dis.* **22**: 355-366.
26. Allen, J. C., J. H. Baxter, and H. C. Goodman. 1961. Effects of dextran, polyvinylpyrrolidone and gamma globulin on the hyperlipidemia of experimental nephrosis. *J. Clin. Invest.* **40**: 499-508.
27. Baxter, J. H., H. C. Goodman, and J. C. Allen. 1961. Effects of infusions of serum albumin on serum lipids and lipoproteins in nephrosis. *J. Clin. Invest.* **40**: 490-498.
28. Glass, C. K., R. C. Pittman, G. A. Keller, and D. Steinberg. 1983. Tissue sites of degradation of apolipoprotein A-I in the rat. *J. Biol. Chem.* **259**: 7161-7167.
29. Sorci-Thomas, M., M. M. Prack, N. Dashfi, F. Johnson, L. L. Rudel, and D. L. Williamson. 1988. Apolipoprotein (apo) A-I production and mRNA abundance explain plasma apolipoprotein A-I and high density lipoprotein differences between two nonhuman primate species with high and low susceptibilities to diet-induced hypercholesterolemia. *J. Biol. Chem.* **263**: 5183-5189.
30. Hughes, T. E., B. F. Nottage, M. D. Mone, and J. R. Paterniti, Jr. 1990. Apolipoprotein A-I production is controlled at the mRNA level in transgenic mice and three cell lines. *Arteriosclerosis.* **10**: 774a.
31. Rubin, E. M., R. M. Krauss, E. A. Spangler, J. G. Verstuyft, and S. M. Clift. 1991. Inhibition of early atherogenesis in transgenic mice by human apolipoprotein A-I. *Nature (London)* **353**: 265-267.
32. Appel, G. B., C. B. Blum, S. Chien, C. L. Kunis, and A. S. Appel. 1985. The hyperlipoproteinemia of the nephrotic syndrome: relation to plasma albumin concentration, oncotic pressure, and viscosity. *N. Engl. J. Med.* **312**: 1544-1548.
33. Verkade, H. J., D. G. Fast, A. E. Rusinol, D. G. Scraba, and D. E. Vance. 1993. Impaired biosynthesis of phosphatidylcholine causes a decrease in the number of very low density lipoprotein particles in the Golgi but not in the endoplasmic reticulum of rat liver. *J. Biol. Chem.* **268**: 24990-24996.
34. Burkey, B. F., N. Vlasic, D. France, T. E. Hughes, M. Drelich, X. Ma, M. B. Stemerman, and J. R. Paterniti. 1992. Elevated apolipoprotein A-I (apolipoprotein A-I) pools in human apolipoprotein A-I transgenic rats decreases aortic smooth muscle cell proliferation following balloon angioplasty. *Circulation.* **86**: 1-472.
35. Ross, R. 1993. The pathogenesis of atherosclerosis: a perspective for the 1990s. *Nature.* **362**: 801-809.
36. Diamond, J. R., G. Ding, J. Frye, and I-P. Diamond. 1992. Glomerular macrophages and the mesangial proliferative response in the experimental nephrotic syndrome. *Am. J. Pathol.* **141**: 887-894.